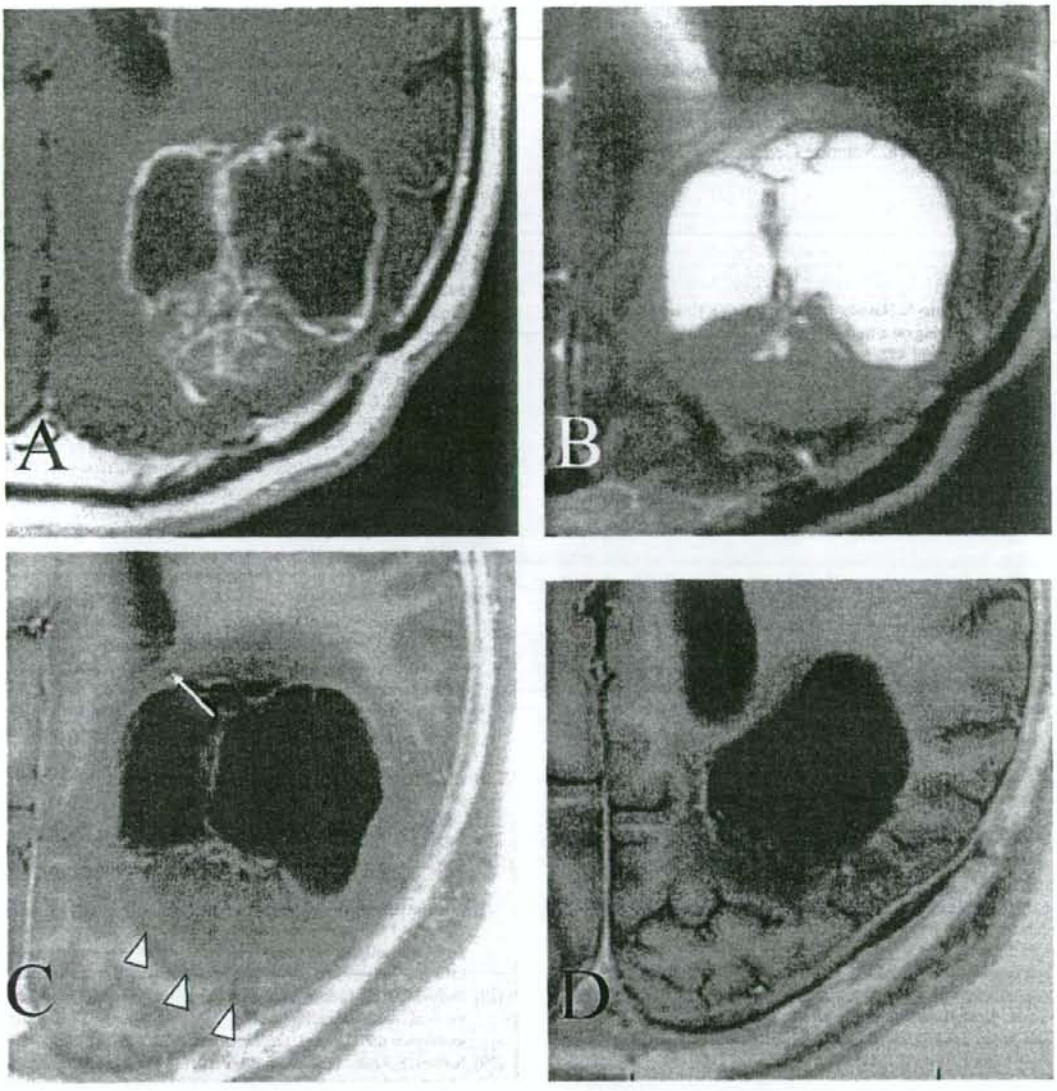

Fig. 3. Images for Case 7. Axial Gd-T1WI using 1.5 T MRI (A) and T2WI using 1.5 T MRI (B). (C) STIR using 3.0 T MRI more clearly demonstrates the parieto-occipital sulcus (arrowheads) separating the tumor from the occipital lobe, and the tumor margin behind the lateral ventricle (arrow), than T2WI. (D) Postoperative STIR shows complete removal of the tumor bulk and preservation of the parietal cortex.

to be split in the trans-sulcal approach to the tumor bulk prior to surgery. We believe that high contrast STIR imaging is suitable for preoperative evaluation of superficially located oligodendroglial tumors.

5. Conclusion

This study demonstrates the usefulness of STIR in brain tumor surgery. Our results, although derived from a small sample size and without comparing the STIR sequence fairly and rigorously with other MRI sequences using the same system, support the recommendation that STIR should become a preoperative examination for the removal of superficially located glioma. The benefits of STIR imaging include: (i) clear depiction of cortical surface structures, and (ii) fine contrast of intra-axial structures, from which the limitations of tumor resection can be evaluated. We believe that STIR is of great assistance to neurosurgeons planning surgical treatment for patients with superficially located glioma.

Acknowledgements

We thank Prof. Nakazato Y, Department of Human Pathology, Gunma University, for his co-operation with pathological diagnoses. This study was supported in part by the Advanced Medical Science Center, Iwate Medical University.

References

[1] Fujii Y, Nakayama N, Nakada T. High-resolution T2-reversed magnetic resonance imaging on a high magnetic field system. Technical note. J Neurosurg 1998;89:492–5.
[2] Sasaki M, Inoue T, Tohyama K, Oikawa H, Ehara S, Ogawa A. High-field MRI of the central nervous system: current approaches to clinical and microscopic imaging. Magn Reson Med Sci 2003;2:133–9.
[3] Harada A, Fujii Y, Yoneoka Y, Takeuchi S, Tanaka R, Nakada T. High-field magnetic resonance imaging in patients with moyamoya disease. J Neurosurg 2001;94:233–7.
[4] Mikami C, Inoue T, Ogasawara K, Ogawa A. Medullary streaks in a patient with atherosclerotic internal carotid artery occlusion: case report. Surg Neurol 2004;62:42–4.
[5] Baur A, Bartl R, Pellengahr C, Baltin V, Reiser M. Neovascularization of bone marrow in patients with diffuse multiple myeloma: a correlative study of magnetic resonance imaging and histopathologic findings. Cancer 2004;101:2599–604.
[6] Cayi SR, Kocak A, Alkan A, Kirimliogclu H. Is there a clinical correlate to the histological and radiological evidence of inflammation in trans-ligamentous extruded and sequestered lumbar disc herniaton? Br J Neurosurg 2004;18:576–83.
[7] Dwyer AJ, Frank JA, Sank VJ, Reinig JW, Hickey AM, Doppman JL. Short-TI inversion-recovery pulse sequence: analysis and initial experience in cancer imaging. Radiology 1988;168:827–36.
[8] Fleckenstein JL, Archer BT, Barker BA, Vaughan JT, Parkey RW, Peshock RM. Fast short-tau inversion-recovery MR imaging. Radiology 1991;179:499–504.
[9] Hickman SJ, Toosy AT, Jones SJ, Altmann DR, Miszkiel KA, MacManus DG, et al. A serial MRI study following optic nerve mean area in acute optic neuritis. Brain 2004;127:2498–505.
[10] Lim R, Jaramillo D, Poussaint TY, Chang Y, Korf B. Superficial neurofibroma: a lesion with unique MRI characteristics in patients with neurofibromatosis Type 1. AJR Am J Roentgenol 2005;184:962–8.
[11] Inoue T, Ogasawara K, Beppu T, Ogawa A. Three-dimensional anisotropy contrast imaging of gliomatosis cerebri: two case reports. Surg Neurol 2004;62:154–5.
[12] Oikawa H, Sasaki M, Tamakawa Y, Ehara S, Tohyama K. The substantia nigra in Parkinson disease: proton density-weighted spin-echo and fast short inversion time inversion-recovery MR findings. AJNR Am J Neuroradiol 2002;23:1747–56.
[13] Sawaishi Y, Sasaki M, Yano T, Hirayama A, Akabane J, Takada G. A hippocampal lesion detected by high-field 3 Tesla magnetic resonance imaging in a patient with temporal lobe epilepsy. Tohoku J Exp Med 2005;205:287–91.
[14] Ellis TL, Stieber VW, Austin RC. Oligodendroglioma. Curr Treat Options Oncol 2003;4:479–90.
[15] Piepmeier J, Baehring JM. Surgical resection for patients with benign primary brain tumors and low grade gliomas. J Neurooncol 2004;69:55–65.
[16] Reinacher PC, van Velthoven V. Intraoperative ultrasound imaging: practical applicability as a real-time navigation system. Acta Neurochir Suppl 2003;85:89–93.
[17] Benveniste R, Germano IM. Evaluation of factors predicting accurate resection of high-grade gliomas by using frameless image-guided stereotactic guidance. Neurosurg Focus 2003;15(14(2)):e5.
[18] Rutten GJ, Ramsey N, Noordmans HJ, Willems P, van Rijen P, Berkelbach van der Sprenkel JW, et al. Toward functional neuronavigation: implementation of functional magnetic resonance imaging data in a surgical guidance system for intraoperative identification of motor and language cortices. Technical note and illustrative case. Neurosurg Focus 2003;15(15(1)):E6.
[19] Nimsky C, Ganslandt O, von Keller B, Fahlbusch R. Intraoperative high-field MRI: anatomical and functional imaging. Acta Neurochir Suppl 2006;98:87–95.
[20] Muragaki Y, Iseki H, Maruyama T, Kawamata T, Yamane F, Nakamura R, et al. Usefulness of intraoperative magnetic resonance imaging for glioma surgery. Acta Neurochir Suppl 2006;98:67–75.
[21] Daumas-Duport C, Tucker ML, Kolles H, Cervera P, Beuvon F, Varlet P, et al. Oligodendrogliomas. Part II: A new grading system based on morphological and imaging criteria. J Neurooncol 1997;34:61–7.
[22] Ricci PE, Dungan DH. Imaging of low- and intermediate-grade gliomas. Semin Radiat Oncol 2001;11:103–12.
[23] Kleihues P, Cavenee WK. World Health Organization classification of tumours: pathology & genetics: tumours of the nervous system. Lyon: International Agency for Research on Cancer (IARC); 2000, 57 pp.
[24] Shuman WP, Griffin BR, Haynor DR, Jones DC, Johnson JS, Cromwell LD, et al. The utility of MR in planning the radiation therapy of oligodendroglioma. AJR Am J Roentgenol 1987;148:595–600.
[25] Celli P, Nofrone BSC, Palma L, Cantore G, Fortuna A. Cerebral oligodendroglioma: prognostic factors and life history. Neurosurgery 1994;35:1018–35.
[26] DeAngelis LS, Gutin PH, Leibel SA, Posner JB. Intracranial tumors: diagnosis and treatment. Oligodendroglial tumors. London: Mattin Dunitz, Ltd.; 2002. pp. 168–72.
[27] Jeremic B, Milicic B, Grujicic D, Samardzic M, Antunovic V, Dagovic A, et al. Combined treatment modality for anaplastic oligodendroglioma and oligoastrocytoma: a 10-year update of a phase II study. Int J Radiat Oncol Biol Phys 2004;59:509–14.
[28] Puduvalli VK, Hashmi M, McAllister LD, Levin VA, Hess KR, Prados M, et al. Anaplastic oligodendrogliomas: prognostic factors for tumor recurrence and survival. Oncology 2003;65:259–66.
[29] Ribom D, Smits A, Hartman M, Persson L, Blomquist E. On the issue of early and aggressive treatment in grade 2 gliomas. J Cancer Res Clin Oncol 2003;129:154–60.
[30] Shaw EG, Scheithauer BW, O'Fallon JR, Tazelaar HD, Davis DH. Oligodendrogliomas: the Mayo Clinic experience. J Neurosurg 1992;76:428–34.
[31] Yasargil MG. Microneurosurgery IV A (in 4 volumes). Case 2. Stuttgart/New York: Georg Thieme Verlag (for distribution in Japan: Nankodo Company, Tokyo); 1993, 158 pp.

Low-Grade Glioma on Stereotactic Biopsy: How Often is the Diagnosis Accurate?

Authors: Y. Muragaki[1, 2], M. Chernov[1], T. Maruyama[1], T. Ochiai[1], T. Taira[1], O. Kubo[1], R. Nakamura[2, 3], H. Iseki[1, 2, 3], T. Hori[1], K. Takakura[1, 2, 3]

Affiliations: Affiliation addresses are listed at the end of the article

Key words
- stereotactic biopsy
- diagnostic accuracy
- low-grade glioma
- MIB-1 index

Abstract

The objective of the present study was an evaluation of the incidence and risk factors for erroneous histopathological diagnosis of low-grade glioma after stereotactic biopsy. Twenty-eight tumors diagnosed as low-grade glioma after stereotactic biopsy and surgically resected thereafter were analyzed. There were 13 astrocytomas, 7 oligodendrogliomas, and 8 mixed gliomas. All neoplasms had a lobar location. Seven tumors had contrast enhancement on MRI. The number of tissue samples obtained during stereotactic biopsy was one in 19 cases, two in 4, and three or more in 5. Complete diagnostic agreement in tumor typing and grading after stereotactic biopsy and surgical resection was attained in 10 cases (36%). Agreement in tumor typing was marked in 16 cases (57%). Erroneous typing was more frequent in tumors with an MIB-1 index of less than 3% ($P = 0.0629$) and mixed gliomas ($P = 0.0801$). Overgrading of WHO grade I tumors was marked in 3 cases (11%) and undergrading of WHO grade III gliomas in 8 cases (28%). Tumor undergrading was more frequent in cases with an MIB-1 index of more than 3% ($P = 0.0045$). The MIB-1 index detected after stereotactic biopsy was nearly always lower compared with those established after surgical resection ($P < 0.0001$). In conclusion, the histopathological diagnosis of low-grade glioma established after stereotactic biopsy is associated with a substantial risk of inaccuracy. Tumors with low proliferative activity and mixed gliomas are especially susceptible for erroneous tumor typing. Undergrading of high-grade gliomas may be suspected if the MIB-1 index in the tumor specimen constitutes more, than 3%.

Bibliography
DOI 10.1055/s-0028-1082322
Minim Invas Neurosurg 2008; 51: 275–279

ISSN 0946-7211

Correspondence
Y. Muragaki, MD, PhD
Faculty of Advanced Techno-Surgery
Institute of Advanced Biomedical Engineering and Science
Graduate School of Medicine
Tokyo Women's Medical University
8-1 Kawada-cho
Shinjuku-ku
Tokyo 162-8666
Japan
Tel.: +81/3/3353 81 11 ext. 399 89
Fax: +81/3/5361 77 96
ymuragaki@abmes.twmu.ac.jp

Introduction

Image-guided stereotactic biopsy represents a standard neurosurgical technique, routinely used in cases of parenchymal brain lesions. Tissue sampling from the area that looks the most abnormal on CT and/or MRI, results in a high rate of positive histopathological findings [1–3]. Nevertheless, heterogeneity of the lesion, frequently observed in gliomas, limits the diagnostic accuracy of the procedure, and not infrequently leads to erroneous tumor typing and/or grading [1, 3–8]. In a large cohort of patients with malignant gliomas diagnosed with stereotactic biopsy a disproportionally greater number of anaplastic astrocytomas compared to glioblastomas was found, which could result from frequent tumor undergrading [4]. In our own series (unpublished data), undergrading of the non-enhancing malignant gliomas represented the most typical histopathological error, which can certainly result in an inappropriate choice of the management strategy and a wrong determination of the prognosis. Therefore, the present analysis was conducted with the objective to identify the incidence and risk factors for erroneous tumor typing and grading in cases of low-grade glioma diagnosed with frame-based image-guided stereotactic biopsy.

Methods and Materials

From January 1, 2002 to December 31, 2006, 69 frame-based image-guided stereotactic biopsies of parenchymal brain lesions were performed in the Department of Neurosurgery of the Tokyo Women's Medical University. In 36 cases the diagnosis of low-grade glioma was established on the permanent histopathological sections. Among the latter, 28 tumors were surgically resected within a month after initial tissue sampling, and represented the

clinical basis of the present study. All analyzed data were extracted from the constantly maintained surgical, pathological, and radiological databases.

Clinical characteristics of patients

No one patient had undergone previous treatment for brain tumor. Their ages varied from 8 to 60 years (mean: 33 ± 13 years; median: 32 years). There were 18 men and 10 women. All lesions were located in the cerebral lobe, mainly frontal (14 cases) and temporal (12 cases). Overall, 15 neoplasms were located on the left side and 13 on the right side. The majority of the tumors (25 cases) had low intensity signal on T_1-, and high intensity signal on T_2-weighted MRI. According to MRI, the structure of the lesion was considered as homogeneous in 14 cases and heterogeneous in 14 cases. Contrast enhancement was present in 7 tumors, and was characterized as heterogeneous in 5 and patchy in two.

Indications and technique of stereotactic biopsy

The main indication for stereotactic biopsy in the present series was the establishment of the histological type and grade of the suspected glioma for scientifically based consideration of the rationale for aggressive tumor resection and detailed information for the patient and his/her family about the prognosis. The procedure was usually accompanied by implantation of the deep brain electrodes for preoperative brain mapping. In each case informed consent was obtained from the patient and his or her nearest family member.

The technique of stereotactic biopsy of parenchymal brain lesions used in the Tokyo Women's Medical University can be briefly presented as follows. On the day of treatment a Leksell G stereotactic frame (Elekta Instruments AB, Stockholm, Sweden) was fixed on the patient's head, the coordinate frame was attached, CT, MRI, and, sometimes, angiography and multivoxel proton magnetic resonance spectroscopy (^{1}H-MRS) were obtained in stereotactic conditions, and all images were transferred for co-registration to the Leksell GammaPlan version 2.0 or, later, Leksell SurgiPlan Release 2.20 (Elekta Instruments AB, Stockholm, Sweden). The contrast-enhanced part of the lesion, or its center, in cases of non-enhancing pathologies, was selected for tissue sampling. In cases of ^{1}H-MRS-supported biopsy the target was chosen within the lesion-containing subvoxels, which had the lowest NAA/Cho ratio. Tissue samples were obtained using a Sedan-type blunt side-cutting aspiration biopsy needle, and were divided in two parts for intraoperative and permanent histopathological investigation. If examination of the frozen biopsy sections did not determine the neoplastic tissue, the sampling was usually repeated. The number of obtained biopsy specimens was one in 19 cases, two in 4, three in 2, four in 2, and nine in 1 case. All procedures were performed under local anesthesia with additional intravenous sedation.

Surgical resection of the tumor

All patients underwent surgical resection of the tumor directed on its maximal possible removal. This was done on average 2 + 1 weeks after initial tissue sampling. Intraoperative MRI, real-time neuronavigation, neurophysiological monitoring, comprehensive brain mapping, awake craniotomy, chemical neuronavigation with 5-aminolevulinic acid, and intraoperative histopathological monitoring of the resected tissue, were used routinely as appropriate. The tumor resection rate varied from 85 to 100%.

Histopathological diagnosis

All histopathological examinations were performed by one neuropathologist. As is noted above, in each case, both during stereotactic biopsy and surgical resection of the tumor, intraoperative examination of the frozen sections was done using hematoxylin and eosin staining. Permanent histopathological examination of the formalin-fixed paraffin-embedded tissue was performed using hematoxylin and eosin staining, as well as appropriate immunohistochemistry. Determination of the MIB-1 index was done in all cases. Typing and grading of intracranial tumors were based on the World Health Organization (WHO) criteria [9]. For diagnosis of oligoastrocytoma the presence of both astrocytic and oligodendroglial components should constitute not less, than 25% [10], otherwise the diagnosis of glioma with specific cell components was made.

Complete diagnostic agreement was considered if the final histopathological diagnoses after both stereotactic biopsy and surgical resection of the tumor were identical, *minor disagreement*, if those were slightly different, but without significant impact on the treatment strategy, and *major disagreement* if histopathological diagnoses differed significantly, which could have a serious impact on the choice of the appropriate management and determination of prognosis [11].

Statistics

The chi-square test with continuity correction, Mann-Whitney test, and Wilcoxon signed rank test were done. The level of significance was determined at $P<0.05$.

Results

Histopathological diagnosis after stereotactic biopsy

The definitive histopathological diagnosis with determination of both type and grade of the tumor was established on the permanent sections after stereotactic biopsy in 22 cases (79%). Astrocytic neoplasms were diagnosed in 13 cases, oligodendrogliomas in 6 cases, including one with an astrocytic component, and oligoastrocytomas in 3 cases. In 6 other patients (21%) an incomplete diagnosis was made, namely low-grade glioma without detailed clarification of the tumor type. The MIB-1 index varied from 0% to 8% (mean: 2.7 ± 2.2%; median: 1.9%). In 8 cases it was less, than 1%, in 9 between 1 and 3%, and in 11 it was more than 3%. All cases were designated as WHO grade II tumors.

Histopathological diagnosis after surgical resection of the tumor

After surgical resection of the tumor, astrocytic neoplasms were diagnosed in 13 cases, including two with oligodendroglial component, oligodendrogliomas in 7 cases, including five with astrocytic components, and mixed gliomas in 8 cases (five oligoastrocytomas, two dysembryoplastic neuroepithelial tumors, and one ganglioglioma with astrocytic and oligodendroglial components). The MIB-1 index varied from 0.5% to 15.7% (mean: 6.7 ± 4.5%; median: 5.8%). Three tumors (11%) were designated as WHO grade I, 17 (60%) as WHO grade II, and 8 (28%) as WHO grade III.

Diagnostic agreement and concordance in tumor typing, grading, and MIB-1 labeling

Complete agreement in tumor typing and grading after stereotactic biopsy and surgical resection was marked in 10 cases

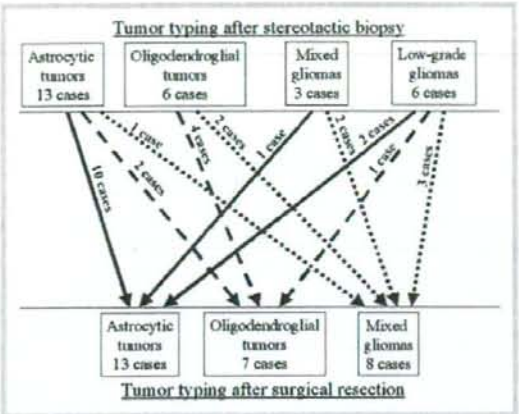

Fig. 1 Correspondence of the histopathological tumor typing after stereotactic biopsy of glioma to that after its surgical resection.

(36%). Minor disagreement was marked in 10 cases (36%) and included initial overgrading of WHO grade I tumors, as well as incomplete histopathological diagnosis or erroneous typing of the low-grade tumor after stereotactic biopsy. Major disagreement was marked in 8 (28%) cases with initial undergrading of WHO grade III glioma. No one investigated factor had a statistically significant association with the attainment of complete diagnostic agreement between stereotactic biopsy and surgical resection.

Concordance in tumor typing after stereotactic biopsy and surgical resection (© Fig. 1) was attained in 16 cases (57%). It had borderline associations with the MIB-1 index established after stereotactic biopsy (P=0.0629) and tumor histological type (P=0.0801). Erroneous typing or incomplete diagnosis after stereotactic biopsy was done in 10 out of 17 cases with an MIB-1 index of less than 3%, and in 2 out of 11 cases with an MIB-1 index of more than 3% (odds ratio: 6.43; 95% confidence interval: 1.05–39.33), as well as in 6 out of 8 mixed gliomas and 6 out of 20 "pure" astrocytic tumors or oligodendrogliomas (odds ratio: 7.00; 95% confidence interval: 1.09–45.15).

Undergrading of WHO grade III tumors was associated with the MIB-1 index established after stereotactic biopsy (P=0.0045). Tumor undergrading was done in 1 out of 17 cases with an MIB-1 index of less than 3%, and in 7 out of 11 cases with an MIB-1 index of more than 3% (odds ratio: 28.00; 95% confidence interval: 2.63–297.67).

The MIB-1 index established after stereotactic biopsy was nearly always lower than those one, which was established after tumor resection (P<0.0001), and in 6 cases (21%) the difference was statistically significant. No one investigated factor had an association with erroneous MIB-1 labeling after stereotactic biopsy.

Discussion

Low-grade gliomas are encountered with an approximate incidence of 0.56–1.03 per 100000 persons per year [12,13]. These tumors are usually manifested between the second and fourth decades of life with seizures, headache, hemiparesis, and mental abnormalities [14–16]. Typical MRI findings include signal hypointensity on T_1- and hyperintensity on T_2-weighted images, absence of the prominent peritumoral edema, mass effect, distant tumor foci, hemorrhage, and necroses [15,17,18]. Absence of contrast enhancement is neither a sensitive, nor a specific sign of low-grade neoplasms. The latter are enhanced in 18–47% of cases, whereas malignant tumors, mainly anaplastic astrocytomas, comprise from 12% to 45% of non-enhancing gliomas [5,16,19–23]. Overall, conventional MRI has limited accuracy in the differentiation of low- and high-grade neuroepithelial brain tumors, which necessitates the use of perfusion-weighted imaging (PWI), positron emission tomography (PET), and ^{1}H-MRS [18,24–26]. Anyway, modern neuroimaging could not substitute the histopathological investigation of the tissue samples, which at present represents the "gold standard" in the diagnosis of brain tumor, its typing and grading [15,19].

Stereotactic brain biopsy is routinely used for the histopathological evaluation of parenchymal brain tumors and their differentiation with non-neoplastic lesions. Determination of the type and grade of the tumor performed with stereotactic biopsy has been frequently considered equal to the diagnosis established after surgical resection of the neoplasm [1,27–29]. Since the rationale for aggressive surgery of gliomas has not been formally proved up to date, the results of stereotactic biopsy are frequently used for the choice of the optimal treatment strategy, determination of prognosis, and usually accepted as a sufficient criterion for case inclusion into the clinical trial [16,23,30]. It makes the preciseness of the histopathological diagnosis established after stereotactic biopsy of paramount importance, but, in fact, in 3–49% of cases it more or less significantly differs from those one which was determined after subsequent tumor removal [1–3,5–8,11,17,31–33]. Complete diagnostic agreement, defined as identical determination of the tumor type and grade after stereotactic biopsy and surgical resection, was marked just in 36% of cases in the present series.

Erroneous tumor typing after stereotactic biopsy of suspected low-grade gliomas was done in 43% of the cases. Oligoastrocytomas and mixed neuronal-glial tumors were especially susceptible for such diagnostic inaccuracy. It is highly possible, that in such cases small tumor specimens could not permit one to evaluate the representation of the different cell types [3,4,34]. From another hand, inaccurate determination of mixed gliomas can be caused by differences in the existing criteria for their morphological characterization and differentiation from "pure" astrocytomas and oligodendrogliomas [9,14]. In the present series, representation of the astrocytic and oligodendroglial components required for the diagnosis of oligoastrocytoma, should constitute at least 25%, whereas others used lower cutoff levels of 20% [16], 10% [14], and even 1% [30]. While inaccurate typing of glioma after stereotactic biopsy is usually considered as a "minor" diagnostic error [1,11], the precise determination of the tumor type may be important for prediction of possible tumor re-growth and malignant progression, response to treatment, and patient survival [4,12–14,16,30]. Moreover, taking into account that the presence of oligodenroglial components in glioma may be associated with a better response to chemotherapy [14,16,23,30], an imprecise determination of the tumor type attained after stereotactic biopsy can potentially influence the results of clinical trials [4].

Tumor undergrading represents the main cause of major diagnostic errors after stereotactic biopsy of glioma and can result in an inappropriate choice of therapy and determination of prognosis [4–6,34]. Misinterpretation of the biopsy findings is especially great in cases of intermediate grade tumors, which is

extremely important for clinical decision-making [35]. In the present study 28% of low-grade gliomas diagnosed with stereotactic biopsy in fact represented WHO grade III tumors. It was proposed that for avoidance of such misdiagnosis the Daumas-Duport grading system should be applied [2,36]. The presence of prominent nuclear atypia, mitoses, or microvascular proliferation in the biopsy sample may be considered as an indirect sign of possible higher tumor grade [14,36]. In the present series proliferative activity determined in the tumor specimen after stereotactic biopsy of the "low-grade glioma" was associated with the probability of tumor undergrading. Heterogeneity of the Ki-67 labeling index within a tumor is somewhat independent from its histological heterogeneity, and proliferative activity is frequently elevated even in those areas of high-grade tumors which do not exhibit microscopic features of anaplasia [34]. It should be taken into account during evaluation of the histopathological data obtained with stereotactic biopsy, and according to our data, tumor undergrading should be strongly suspected if the MIB-1 index of the otherwise "low-grade glioma" constitutes more than 3%.

Surprisingly, in the present series the MIB-1 index established after stereotactic brain biopsy was nearly always lower, compared to those one, which was established after surgical resection of the neoplasm, and in 21% of cases this difference was statistically significant. Heterogeneity of Ki-67 expression in gliomas is well known [34]. It can be speculated that the contrast-enhanced part of the neoplasm, or its center if contrast enhancement is absent, which are usually used as a target for stereotactic biopsy, might not correspond to the areas of the tumor with the highest proliferative activity.

Multiple tissue sampling from different parts of the neoplasm was proposed for an improvement of the diagnostic accuracy of stereotactic biopsy [2,3,5,27,32,34,36]. In contrast, in the majority of our patients only one tissue specimen was taken for histopathological investigation. In 6 out of 19 such cases (32%) undergrading of malignant glioma was marked, compared to 1 out of 4 cases (25%) when two tissue samples were obtained at the time of biopsy, and 1 out of 5 cases (20%) if three or more tumor specimens were taken. This difference, however, was not statistically significant. Additionally, it should be noted that multiple sampling of the lesion located within the functionally important brain area may result in increased neurological morbidity [3,24]. On the other hand, newest imaging modalities, such as PET [24,26], single photon emission computed tomography [37], ^{1}H-MRS [38,39], and PWI [18,25], can potentially provide better target selection and may result in an improved diagnostic yield of stereotactic biopsy of parenchymal brain tumors. The better diagnostic accuracy of such procedures, however, still needs to be proved.

It seems important that interpretation of the histopathological findings after image-guided frame-based stereotactic biopsy were done with consideration of other factors. Since the risk of malignancy in gliomas is increasing with age [13,20,22], it should be always taken into consideration. On the other hand, characteristics of the tumor obtained with structural, functional, and metabolic neuroimaging can be used as a clue for prediction of its malignant potential [6,17,18,26]. Correspondence of all clinical and neuroradiological data to the histopathological diagnosis of low-grade glioma established after stereotactic biopsy can augment its probability, whereas their discrepancy should raise a suspicion of the possible diagnostic error with corresponding corrections in the treatment strategy and follow-up schedule.

In conclusion, the histopathological diagnosis of low-grade glioma established after stereotactic biopsy of parenchymal brain tumor is associated with a substantial risk of inaccuracy. In the present series, complete diagnostic agreement in determination of type and grade of the neoplasm after stereotactic biopsy and subsequent surgical resection was attained just in 36% of cases. At the same time erroneous tumor typing, undergrading, and inaccurate MIB-1 labeling were marked in 43, 28, and 21% respectively. Tumors with low proliferative activity and mixed gliomas were particularly susceptible for erroneous tumor typing. Undergrading of high-grade tumor may be suspected if the MIB-1 index in the biopsy sample of an otherwise "low-grade glioma" constitutes more than 3%.

Acknowledgements

The authors are thankful to Mr. Takashi Sakayori for his invaluable technical assistance during the present study. This work was supported by the Program for Promoting the Establishment of Strategic Research Centers, Special Coordination Funds for Promoting Science and Technology, Ministry of Education, Culture, Sports, Science and Technology (Japan). Additional support was provided by a grant of the Third Term of the 10-Year-Strategy for Cancer Control from Ministry of Health, Labour and Welfare of Japan, and the Industrial Technology Research Grant Program in 2000–2005 (A45003a) from the New Energy and Industrial Technology Development Organization of Japan (to Dr. Yoshihiro Muragaki).

Affiliations

[1] Department of Neurosurgery, Neurological Institute, Tokyo Women's Medical University, Tokyo, Japan
[2] Faculty of Advanced Techno-Surgery, Institute of Advanced Biomedical Engineering and Science, Tokyo Women's Medical University, Tokyo, Japan
[3] International Research and Educational Institute for Integrated Medical Sciences (IREIIMS), Tokyo Women's Medical University, Tokyo, Japan

References

1 *Chandrasoma PT, Smith MM, Apuzzo MLJ.* Stereotactic biopsy in the diagnosis of brain masses: comparison of results of biopsy and resected surgical specimen. Neurosurgery 1989; 24: 160–165
2 *Revesz T, Scaravilli F, Coutinho L et al.* Reliability of histological diagnosis including grading in gliomas biopsied by image-guided stereotactic technique. Brain 1993; 116: 781–793
3 *Kim JE, Kim DG, Paek SH et al.* Stereotactic biopsy for intracranial lesions: reliability and its impact on the planning of treatment. Acta Neurochir (Wien) 2003; 145: 547–555
4 *Glantz MJ, Burger PC, Herndon JE II et al.* Influence of the type of surgery on the histologic diagnosis in patients with anaplastic gliomas. Neurology 1991; 41: 1741–1744
5 *Grunert P, Ungersbock K, Bohl J et al.* Results of 200 intracranial stereotactic biopsies. Neurosurg Rev 1994; 17: 59–66
6 *Vaquero J, Martinez R, Manrique M.* Stereotactic biopsy for brain tumors: is it always necessary? Surg Neurol 2000; 53: 432–438
7 *Jackson RJ, Fuller GN, Abi-Said D et al.* Limitations of stereotactic biopsy in the initial management of gliomas. Neurooncology 2001; 3: 193–200
8 *MacGirt MJ, Villavicencio AT, Bulsara KR et al.* MRI-guided stereotactic biopsy in the diagnosis of glioma: comparison of biopsy and surgical resection specimen. Surg Neurol 2003; 59: 277–282
9 *Kleihues P, Cavenee WK,* eds. Pathology and genetics of tumours of the Nervous System. Lyon: IARC Press; 2000
10 *Mork SJ, Halvorsen TB, Lindegaard K-F et al.* Oligodendroglioma: histologic evaluation and prognosis. J Neuropathol Exp Neurol 1986; 45: 65–78
11 *Aker FV, Hakan T, Karadereler S et al.* Accuracy and diagnostic yield of stereotactic biopsy in the diagnosis of brain masses: comparison of

results of biopsy and resected surgical specimens. Neuropathology 2005; 25: 207–213
12 *Okamoto Y, Patre PL Di, Burkhard C et al.* Population-based study on incidence, survival rates, and genetic alterations of low-grade diffuse astrocytomas and oligodendrogliomas. Acta Neuropathol (Berl) 2004; 108: 49–56
13 *Ohgaki H, Kleihues P.* Population-based studies on incidence, survival rates, and genetic alterations in astrocytic and oligodendroglial gliomas. J Neuropathol Exp Neurol 2005; 64: 479–489
14 *Krouwer HCJ, Duinen SG van, Kamphorst W et al.* Oligoastrocytomas: a clinicopathological study of 52 cases. J Neurooncol 1997; 33: 223–238
15 *Grier JT, Batchelor T.* Low-grade gliomas in adults. Oncologist 2006; 11: 681–693
16 *Lebrun C, Fontaine D, Bourg V et al.* Treatment of newly diagnosed symptomatic pure low-grade oligodendrogliomas with PCV chemotherapy. Eur J Neurol 2007; 14: 391–398
17 *Dean BL, Drayer BP, Bird CR et al.* Gliomas: classification with MR imaging. Radiology 1990; 174: 411–415
18 *Law M, Yang S, Wang H et al.* Glioma grading: sensitivity, specificity, and predictive values of perfusion MR imaging and proton MR spectroscopic imaging compared with conventional MR imaging. AJNR Am J Neuroradiol 2003; 24: 1989–1998
19 *Kondziolka D, Lunsford LD, Martinez AJ.* Unreliability of contemporary neurodiagnostic imaging in evaluating suspected adult supratentorial (low-grade) astrocytoma. J Neurosurg 1993; 79: 533–536
20 *Barker FG II, Chang SM, Huhn SL et al.* Age and the risk of anaplasia in magnetic resonance-nonenhancing supratentorial cerebral tumors. Cancer 1997; 80: 936–941
21 *Ginsberg LE, Fuller GN, Hashmi M et al.* The significance of lack of MR contrast enhancement of supratentorial brain tumors in adults: histopathological evaluation of a series. Surg Neurol 1998; 49: 436–440
22 *Scott JN, Brasher PMA, Sevick RJ et al.* How often are nonenhancing supratentorial gliomas malignant? A population study. Neurology 2002; 59: 947–949
23 *Buckner JC, Gesme D Jr, O'Fallon JR et al.* Phase II trial of procarbazine, lomustine, and vincristine as initial therapy for patients with low-grade oligodendroglioma or oligoastrocytoma: efficacy and associations with chromosomal abnormalities. J Clin Oncol 2003; 21: 251–255
24 *Massager N, David P, Goldman S et al.* Combined magnetic resonance imaging- and positron emission tomography-guided stereotactic biopsy in brainstem mass lesions: diagnostic yield in a series of 30 patients. J Neurosurg 2000; 93: 951–957
25 *Maia ACM Jr, Malheiros SMF, da Rocha AJ et al.* Stereotactic biopsy guidance in adults with supratentorial nonenhancing gliomas: role of perfusion-weighted magnetic resonance imaging. J Neurosurg 2004; 101: 970–976
26 *Floeth FW, Pauleit D, Wittsack H-J et al.* Multimodal metabolic imaging of cerebral gliomas: positron emission tomography with [^{18}F] fluoroethyl-L-tyrosine and magnetic resonance spectroscopy. J Neurosurg 2005; 102: 318–327
27 *Kelly PJ, Daumas-Duport C, Kispert DB et al.* Imaging-based stereotaxic serial biopsies in untreated intracranial glial neoplasms. J Neurosurg 1987; 66: 865–874
28 *Plunkett R, Allison RR, Grand W.* Stereotactic neurosurgical biopsy is an underutilized modality. Neurosurg Rev 1999; 22: 117–120
29 *Yu X, Liu Z, Tian Z et al.* Stereotactic biopsy for intracranial space-occupying lesions: clinical analysis of 550 cases. Stereotact Funct Neurosurg 2000; 75: 103–108
30 *Kim L, Hochberg FH, Thornton AF et al.* Procarbazine, lomustine, and vincristine (PCV) chemotherapy for Grade III and Grade IV oligoastrocytomas. J Neurosurg 1996; 85: 602–607
31 *Blaauw G, Braakman R.* Pitfalls in diagnostic stereotactic brain surgery. Acta Neurochir Suppl 1988; 42: 161–165
32 *Feiden W, Steude U, Bise K et al.* Accuracy of stereotactic brain tumor biopsy: comparison of the histologic findings in biopsy cylinders and resected tumor tissue. Neurosurg Rev 1991; 14: 51–56
33 *Soo TM, Bernstein M, Provias J et al.* Failed stereotactic biopsy in a series of 518 cases. Stereotact Funct Neurosurg 1996; 64: 183–196
34 *Coons SW, Johnson PC.* Regional heterogeneity in the proliferative activity of human gliomas as measured by the Ki-67 labeling index. J Neuropathol Exp Neurol 1993; 52: 609–618
35 *Mittler MA, Walters BC, Stopa EG.* Observer reliability in histological grading of astrocytoma stereotactic biopsies. J Neurosurg 1996; 85: 1091–1094
36 *Daumas-Duport C, Scheithauer B, O'Fallon J et al.* Grading of astrocytomas: a simple and reproducible method. Cancer 1988; 62: 2152–2165
37 *Hemm S, Vayssiere N, Zanca M et al.* Thallium SPECT-based stereotactic targeting for brain tumor biopsies. Stereotact Funct Neurosurg 2004; 82: 70–76
38 *Son BC, Kim MC, Choi BG et al.* Proton magnetic resonance chemical shift imaging (1H CSI)-directed stereotactic biopsy. Acta Neurochir (Wien) 2001; 143: 45–50
39 *Hall WA, Truwit CL.* 1.5T spectroscopy-supported brain biopsy. Neurosurg Clin N Am 2005; 16: 165–172

ORIGINAL RESEARCH

Metabolic Assessment of Gliomas Using ^{11}C-Methionine, [^{18}F] Fluorodeoxyglucose, and ^{11}C-Choline Positron-Emission Tomography

T. Kato
J. Shinoda
N. Nakayama
K. Miwa
A. Okumura
H. Yano
S. Yoshimura
T. Maruyama
Y. Muragaki
T. Iwama

BACKGROUND AND PURPOSE: Positron-emission tomography (PET) is a useful tool in oncology. The aim of this study was to assess the metabolic activity of gliomas using ^{11}C-methionine (MET), [^{18}F] fluorodeoxyglucose (FDG), and ^{11}C-choline (CHO) PET and to explore the correlation between the metabolic activity and histopathologic features.

MATERIALS AND METHODS: PET examinations were performed for 95 primary gliomas (37 grade II, 37 grade III, and 21 grade IV). We measured the tumor/normal brain uptake ratio (T/N ratio) on each PET and investigated the correlations among the tracer uptake, tumor grade, tumor type, and tumor proliferation activity. In addition, we compared the ease of visual evaluation for tumor detection.

RESULTS: All 3 of the tracers showed positive correlations with astrocytic tumor (AT) grades (II/IV and III/IV). The MET T/N ratio of oligodendroglial tumors (OTs) was significantly higher than that of ATs of the same grade. The CHO T/N ratio showed a significant positive correlation with histopathologic grade in OTs. Tumor grade and type influenced MET uptake only. MET T/N ratios of more than 2.0 were seen in 87% of all of the gliomas. All of the tracers showed significantly positive correlations with Mib-1 labeling index in ATs but not in OTs and oligoastrocytic tumors.

CONCLUSION: MET PET appears to be useful in evaluating grade, type, and proliferative activity of ATs. CHO PET may be useful in evaluating the potential malignancy of OTs. In terms of visual evaluation of tumor localization, MET PET is superior to FDG and CHO PET in all of the gliomas, due to its straightforward detection of "hot lesions".

Positron-emission tomography (PET) can provide valuable metabolic information and is used for grading and characterizing brain tumors, evaluating treatment response, and predicting prognosis. In brain tumors, the 2 most widely used tracers are [^{18}F] fluorodeoxyglucose (FDG) and ^{11}C-methionine (MET). In previous reports, a relationship was found between FDG uptake and glioma grade and between MET uptake and glioma grade.[1-8] FDG allows detection of the increased glucose uptake characteristic of malignant cells, so FDG PET has previously been used successfully in oncology. Recent studies of other organ systems have demonstrated a close correlation with FDG uptake and the proliferative activity of tumors.[9-12] Due to the high-glucose metabolism in normal brain tissue, however, FDG may not be the ideal tracer for detection of gliomas. MET is more appropriate to image the size and spread of gliomas, even without enhancement on contrast-enhanced MR imaging, because MET PET has the advantage of showing selective uptake in the brain tumor compared with normal brain tissue. More recently, ^{11}C-choline (CHO) was introduced as another novel agent to evaluate different aspects of tumors.[13-16]

In both low-grade and high-grade oligodendrogliomas (ODs) increased vascular attenuation was seen, in contrast to astrocytic tumors (ATs), for which microvascular proliferation was seen in only high-grade tumors.[17,18] Using conventional modalities, there are no specific neuroradiologic features that can differentiate between ATs and oligodendroglial tumors (OTs); however, clinical management of OTs differs from other gliomas due to the specific chemotherapeutic sensitivities of OTs.[19,20] We hypothesized that a multitracer investigation that examined pretreatment tumor uptake compared with normal brain would provide valuable information about glioma grade and type; therefore, we studied metabolic activity by using MET, FDG, and CHO PET and compared them with tumor pathology. In addition, we compared the ease with which tumors could be visually evaluated in each system and investigated each tumor's proliferation index, comparing this with the metabolic activity as measured with PET.

Received November 21, 2007; accepted after revision December 26.

From the Chubu Medical Center for Prolonged Traumatic Brain Dysfunction (T.K., J.S., K.M., A.O.), Kizawa Memorial Hospital, Minokamo City, Gifu, Japan; Department of Neurosurgery (T.K., N.N., H.Y., S.Y., T.I.), Gifu University Graduate School of Medicine, Gifu, Japan; and Department of Neurosurgery (T.M., Y.M.), Neurological Institute, Tokyo Women's Medical University, Tokyo, Japan.

Please address correspondence to Takayuki Kato, Chubu Medical Center for Prolonged Traumatic Brain Dysfunction, Kizawa Memorial Hospital, 630 Shimoiotsu, Kobi-machi, and Minokamo City, Gifu, Japan 505-0034; e-mail: itaka1010@gmail.com

DOI 10.3174/ajnr.A1008

Materials and Methods

Patients

From January 1, 2002, through June 30, 2006, we examined the metabolic activity of primary gliomas in 95 patients at the Chubu Medical Center for Prolonged Traumatic Brain Dysfunction, Kizawa Memorial Hospital, in this retrospective study. All of the patients gave written informed consent, and the protocol was approved by the research committee of Kizawa Memorial Hospital Foundation.

PET examinations performed in patients with brain stem gliomas and World Health Organization (WHO) grade I tumors were excluded. We also excluded stereotactic biopsy cases, because histology was occasionally insufficient for definitive tumor grading. All of the patients underwent open surgical procedures within 4 weeks after PET scanning. Presurgical radiologic evaluation was performed with MET PET, FDG PET, CHO PET, and contrast-enhanced MR imaging in all of the patients. We included cases of "the hottest lesion" demonstrated preoperatively on each PET that were resectable. Tumors

Table 1: Histopathologic results according to WHO classification and MRI findings

WHO Classification	No. of Patients	Age, Mean ± SD, y	Tumor Size, Mean ± SD, cm³	MRI Enhancement*		
				None	Weak	Strong
Grade II						
Diffuse astrocytoma	14	37.9 ± 13.4	51.1 ± 44.4	11	1	2
Oligodendroglioma	9	36.8 ± 12.4	65.7 ± 56.7	6	3	0
Oligoastrocytoma	14	38.6 ± 14.1	48.3 ± 41.0	12	1	1
Grade III						
Anaplastic astrocytoma	19	43.2 ± 13.6	48.7 ± 23.3	5	8	6
Anaplastic oligodendroglioma	13	50.2 ± 14.8	40.4 ± 27.6	4	2	7
Anaplastic oligoastrocytoma	5	44.2 ± 18.8	35.2 ± 10.2	3	2	0
Grade IV						
Glioblastoma multiforme	21	60.0 ± 10.9	43.7 ± 32.7	0	3	18
Total	95	45.9 ± 15.6	47.6 ± 35.6	41	20	34

Note:—MRI indicates MR imaging; WHO, World Health Organization.
* None indicates no enhancement; weak, partial or slight enhancement; strong, obvious enhancement.

were classified according to their histologic diagnosis by using the WHO classification. Fifty-four tumors were ATs, 22 were OTs, and 19 were mixed oligoastrocytic tumors (OATs), and all of the tumors were located supratentorially. A summary of these data is shown in Table 1.

PET Scan Procedure

The PET study was carried out according to the standardized procedure used in our institution. The PET scanner was an ADVANCE NXi Imaging System (General Electric Yokokawa Medical System, Hinoshi, Tokyo, Japan), which provides 35 transaxial images at 4.25-mm intervals. The in-plane spatial resolution (full width at half maximum) was 4.8 mm, and the scan mode was the standard 2D mode. Before the emission scan was performed, a 3-minute transmission scan was performed to correct photon attenuation with a ring source containing ^{68}Ge. Patients fasted for at least 4 hours before PET studies. A venous cannula was inserted in the forearm for injection of the radiopharmaceuticals. From this cannula, a blood sample was also drawn to measure the serum glucose level, and blood glucose levels were corrected if necessary. A dose of 7.0 MBq/kg of MET, 5.0 MBq/kg of FDG, or 7.0 MBq/kg of CHO was injected intravenously, depending on the examination. The emission scan was acquired as follows: 1) for 30 minutes, beginning 5 minutes after MET injection; 2) for 7 minutes, beginning 35 minutes after FDG injection; and 3) for 7 minutes, beginning 2 minutes after CHO injection. During PET data acquisition, head motion was continuously monitored by using laser beams projected onto ink markers drawn over the forehead skin and corrected manually, as necessary. The images were reconstructed by using the ordered-subsets expectation maximization algorithm.

MR Imaging Procedure

MR imaging was performed on a 1.5T system (Signa; GE Medical Systems, Milwaukee, Wis). T1-weighted images, T2-weighted images, and fluid-attenuated inversion recovery (FLAIR) images were acquired using our standard protocol. For coregistration of metabolic and anatomic data, 3D spoiled gradient-echo images were also acquired after administration of 0.2 mL/kg of gadopentetate dimeglumine (Gd-DTPA, Magnevist; Nihon Shering, Osaka, Japan) by using following parameters: no gap; 1.0-mm thickness; TR/TE = 20.0/1.6 ms; flip angle = 15°; NEX = 1; and axial views.

Tumor volume was measured using the Gd-DTPA enhanced area. When enhancement was absent, we referred to the FLAIR image. Gd-DTPA enhancement was classified as follows: none, no enhancement; weak, partial or slight enhancement; or strong, obvious enhancement throughout the tumor.

Data Analysis

Tracer accumulation in the regions of interest (ROIs) was analyzed as the standardized uptake value (SUV), which is the activity concentration in the ROI at a fixed time point divided by the injected dose normalized to the patient's measured weight. The MET, FDG, and CHO SUV tumor/normal brain uptake ratios (T/N ratios) were calculated by dividing the maximum SUV for the tumor by the mean SUV of contralateral normal frontal cortex. The tumor SUVs were selected as the highest accumulation, and the reference ROIs were drawn in 3 circular ROIs with a diameter of 10 mm on each of the 3 axial planes. Coregistration of PET and MR imaging was undertaken in all of the cases with the Dr View, an image analysis software package (AJS, Tokyo, Japan), by using a method described by Kapouleas et al.[23] If increased accumulation was absent or not clear, an ROI was selected in consultation with the fusion image. We used the T/N ratio instead of absolute SUV because of the high, unexplained intersubject variability of SUV. We used tumor maximum SUV instead of tumor mean SUV to minimize the effect of tumor heterogeneity. In each tracer we defined the T/N ratios more than 2.0 as hot lesions and carried out analysis of what percentage took in all of the cases to evaluate visual ease for tumor detection.

Proliferation Activity

The tumors were graded according to the WHO classification of brain tumors from representative hematoxylin-eosin-stained slides of each tumor. An avidin-biotin immunoperoxidase or simple stain MAX peroxidase (Nichirei, Tokyo, Japan) technique was used to perform a Mib-1 monoclonal antibody (DAKO, Glostrup, Denmark) assay in selected sections of each case. The Mib-1 labeling index (LI) was quantified visually by counting the number of mitoses in areas of the tumor showing the highest number of immunopositive nuclei. All of the tissue sections were examined at high-power magnification (×400) along horizontal and vertical axes perpendicular to each other until 1000 cells were counted. Only neoplastic cells were included in the quantification of the Mib-1-positive cells. Necrotic and hemorrhagic areas and the borders of each section were omitted from quantification. The results were expressed as the percentage of Mib-1-positive cells per 1000 tumor cells.

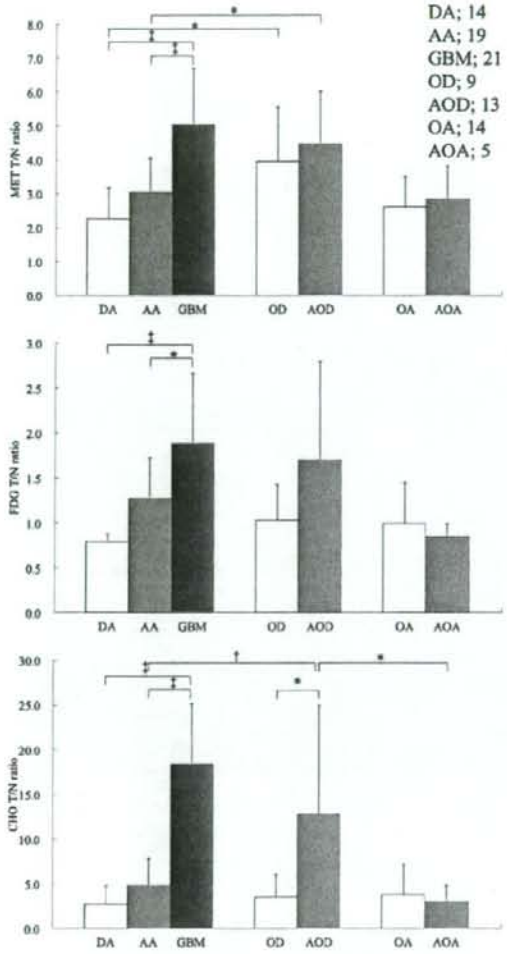

Fig 1. Graph showing the correlation between tracer uptake and tumor grade. *$P < .05$, †$P < .01$, ‡$P < .001$.

Statistical Analysis

Data are presented as means ± SDs. To compare the T/N ratios between histologic grade and type, statistical analyses were performed using analysis of variance and a Tukey post hoc test. Analyses of covariance (ANCOVAs) were used to determine whether tumor-related factors (grade, type, Gd-DTPA enhancement, and tumor size) influenced each tracer uptake. To compare the percentage of the hot lesions among 3 tracers, statistical analyses were performed using χ^2 test with Bonferroni correction. To determine whether tracer accumulations were related to each other and/or to proliferation activity, Spearman correlation coefficients were calculated. *P* values less than .05 were considered statistically significant.

Results

Semiquantitative Analysis of PET Studies

The mean SUVs of the contralateral normal frontal cortex of MET, FDG, and CHO were 1.25 ± 0.39, 6.48 ± 1.51, and 0.29 ± 0.07, respectively. In ATs, MET T/N ratios of diffuse astrocytoma (DA), anaplastic astrocytoma (AA), and glioblastoma multiforme (GBM) were 2.24 ± 0.90, 3.03 ± 1.02, and 5.03 ± 1.65, respectively. There was a significant difference between these ratios among the different grades of ATs (DA/GBM: $P < .001$; AA/GBM: $P < .001$). In OTs and OAs, MET T/N ratios of OD, anaplastic oligodendroglioma (AOD), oligoastrocytoma (OA), and anaplastic oligoastrocytoma (AOA) were 3.95 ± 1.60, 4.46 ± 1.55, 2.60 ± 0.91, and 2.83 ± 0.99, respectively. There were no significant differences between the ratios of OD and AOD or between those of OA and AOA (Fig 1).

In ATs, FDG T/N ratios of DA, AA, and GBM were 0.79 ± 0.08, 1.27 ± 0.46, and 1.88 ± 0.78, respectively. Significant differences were present between the different grades of ATs (DA/GBM: $P < .001$; AA/GBM: $P < .05$). However, no significant differences were seen between FDG T/N ratio of OTs and that of OATs (OD: 1.03 ± 0.40; AOD: 1.71 ± 1.09; OA: 1.00 ± 0.45; AOA: 0.85 ± 0.15; Fig 1).

In ATs, CHO T/N ratios of DA, AA, and GBM were 2.69 ± 2.04, 4.76 ± 3.04, and 18.35 ± 6.73, respectively. Significant differences were present between the different grades of ATs (DA/GBM: $P < .001$; AA/GBM: $P < .001$). In OTs, significantly different CHO T/N ratios were observed between OD and AOD (3.46 ± 2.52 and 12.71 ± 12.21, respectively; $P < .05$). In OAs, CHO T/N ratios of OA and AOA were not significantly different (3.78 ± 3.36 and 3.02 ± 1.74, respectively; Fig 1).

In grade II gliomas, the MET T/N ratio of OD was the highest, and there was a significant difference between the DA and OD ($P < .05$); however, no significant differences were seen on FDG or CHO PET between these 2 tumors. In grade III gliomas, MET and CHO T/N ratios of AOD were the highest, and significant differences were shown between AA and AOD (MET: $P < .05$; CHO: $P < .01$) and between AOA and AOD (CHO: $P < .05$). However, a significant difference was not observed on FDG PET (Table 2 and Fig 1). Representative cases are shown in Fig 2.

Tumor size did not reach statistical significance in each glioma. Tumor size did not appear to affect each tracer uptake by ANCOVAs. Grade influenced all of the tracers, and tumor type influenced MET uptake only. The degree of Gd-DTPA enhancement influenced MET and CHO uptake (Table 3).

Table 2: T/N ratio in gliomas

Tumor	Grade II, Mean ± SD	Grade III, Mean ± SD	Grade IV, Mean ± SD
Astrocytic tumor, *n*	14	19	21
MET	2.24 ± 0.90	3.03 ± 1.02	5.03 ± 1.65
FDG	0.79 ± 0.08	1.27 ± 0.46	1.88 ± 0.78
CHO	2.69 ± 2.04	4.76 ± 3.04	18.35 ± 6.73
Oligodendroglial tumor	9	13	
MET	3.95 ± 1.60	4.46 ± 1.55	
FDG	1.03 ± 0.40	1.71 ± 1.09	
CHO	3.46 ± 2.52	12.71 ± 12.21	
Oligoastrocytic tumor	14	5	
MET	2.60 ± 0.91	2.83 ± 0.99	
FDG	1.00 ± 0.45	0.85 ± 0.15	
CHO	3.78 ± 3.36	3.02 ± 1.74	

Note:—T/N ratio indicates tumor/normal brain uptake ratio; MET, ^{11}C-methionine; FDG, [^{18}F] fluorodeoxyglucose; CHO, ^{11}C-choline.

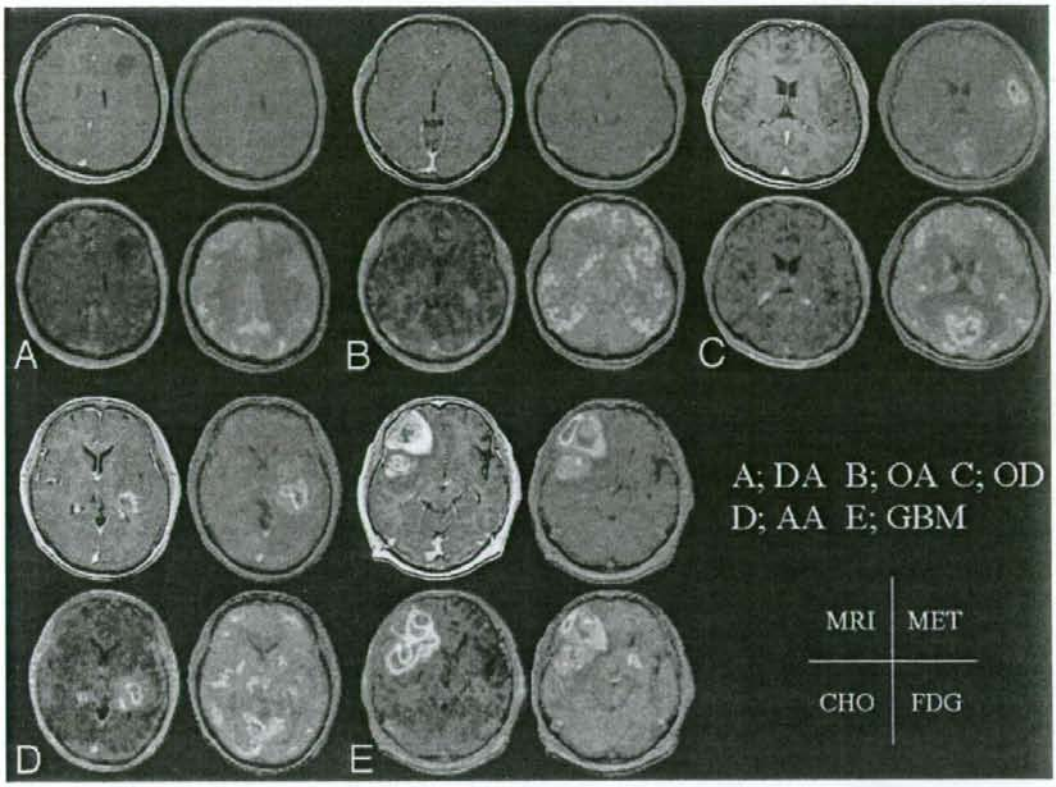

Fig 2. *Left top*, Contrast-enhanced, T1-weighted image. *Right top*, MET PET is superimposed on MR imaging. *Left bottom*, CHO PET is superimposed on MR imaging. *Right bottom*, FDG PET is superimposed on MR imaging. *A*, A 32-year-old woman presented with diffuse astrocytoma. MET T/N ratio = 1.72, CHO T/N ratio = 1.38, and FDG T/N ratio = 0.66. *B*, A 23-year-old woman presented with oligoastrocytoma. MET T/N ratio = 2.76, CHO T/N ratio = 1.82, and FDG T/N ratio = 0.92. *C*, A 44-year-old man presented with oligodendroglioma. MET T/N ratio = 3.71, CHO T/N ratio = 2.74, and FDG T/N ratio = 1.07. *D*, A 62-year-old woman presented with anaplastic astrocytoma. MET T/N ratio = 4.26, CHO T/N ratio = 10.17, and FDG T/N ratio = 1.24. *E*, A 68-year-old man presented with glioblastoma multiforme. MET T/N ratio = 6.85, CHO T/N ratio = 33.38, and FDG T/N ratio = 2.55.

Table 3: Summary statistics of ANCOVAs

Variable	MET, *P*	FDG, *P*	CHO, *P*
Size	.07	.39	.19
Grade	< .005	< .005	< .001
Type	< .05	.33	.12
Gd-DTPA enhancement	< .05	.30	< .01

Note:—MET indicates ^{11}C-methionine; FDG, [^{18}F] fluorodeoxyglucose; CHO, ^{11}C-choline; Gd-DTPA, gadopentetate dimeglumine.

Table 4: Percentage of T/N ratio more than 2.0 in gliomas

Variable	Grade II (37), *n* (%)	Grade III (37), *n* (%)	Grade IV (21), *n* (%)	Overall (95), *n* (%)*
MET	28 (75.7)	34 (91.9)	21 (100.0)	83 (87.4)
FDG	1 (2.7)	6 (16.2)	6 (28.6)	13 (13.7)
CHO	18 (48.6)	29 (78.4)	21 (100.0)	68 (71.6)

Note:—T/N ratio indicates tumor/normal brain uptake ratio; MET, ^{11}C-methionine; FDG, [^{18}F] fluorodeoxyglucose; CHO, ^{11}C-choline.
* There were significant differences in the percentage of T/N ratio more than 2.0 among 3 tracers by using χ^2 test with Bonferroni correction (MET/FDG and CHO/FDG: $P < .001$; MET/CHO: $P < .01$).

Visual Evaluation for Tumor Localization

The T/N ratio of MET was more than 2.0 in 75.7% of grade II, 91.9% of grade III, 100% of grade IV, and 87.4% of all of the gliomas. The T/N ratio of CHO was more than 2.0 in 48.6% of grade II, 78.4% of grade III, 100% of grade IV, and 71.6% of all of the gliomas. The T/N ratio of FDG was more than 2.0 in 2.7% of grade II, 16.2% of grade III, 28.6% of grade IV, and 13.7% of all gliomas (Table 4). In all of the gliomas, the percentage of hot lesions was the highest on MET PET, and there were significant differences in the percentage of hot lesions among 3 tracers (MET/FDG and CHO/FDG: $P < .001$; MET/CHO: $P < .01$).

Correlation Among 3 Tracer Accumulations

In all of the gliomas, significant correlations among the T/N ratios of MET, FDG, and CHO were shown (Fig 3). Significant correlations were also shown between ATs and OTs (ATs: MET/FDG: $r = 0.68$, MET/CHO: $r = 0.83$, FDG/CHO: $r = 0.67$; OTs: MET/FDG: $r = 0.66$, MET/CHO: $r = 0.81$, FDG/CHO: $r = 0.81$; $P < .001$ for each). In OATs, significant correlations were observed between FDG and CHO ($r = 0.67$; $P < .005$) and between MET and FDG ($r = 0.58$; $P < .01$) but not between MET and CHO ($r = 0.40$; $P = .09$).

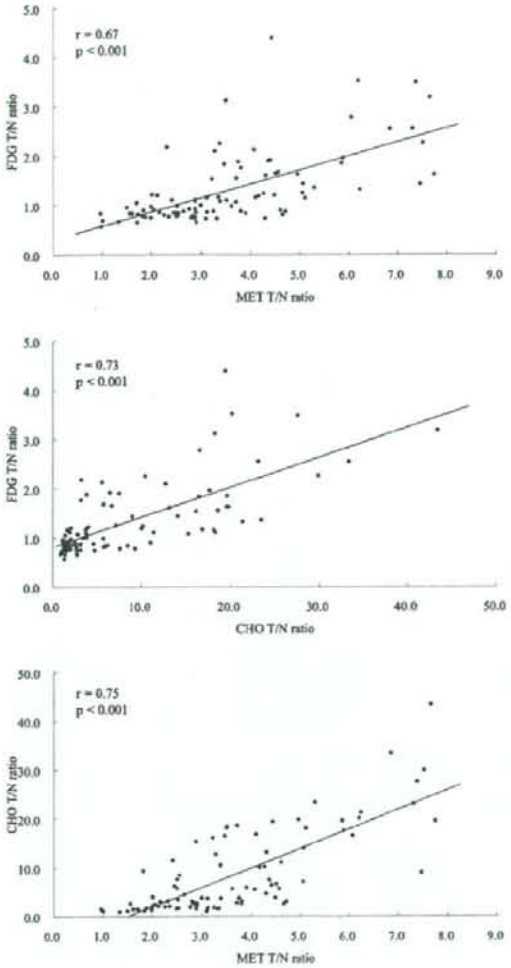

Fig 3. Graph showing the correlation between MET T/N ratio and FDG T/N ratio ($r = 0.67$; $P < .001$), CHO T/N ratio and FDG T/N ratio ($r = 0.73$; $P < .001$), and MET T/N ratio and CHO T/N ratio ($r = 0.75$; $P < .001$) in all of the gliomas.

Table 5: Correlation between tracer uptake and proliferation index

		Mib-1 LI	
Variable	Tumor	*P*	*r*
MET	Astrocytic tumor	< .001	0.64
	Oligodendroglial tumor	.63	−0.13
	Oligoastrocytic tumor	.84	0.05
	All tumor	< .01	0.31
FDG	Astrocytic tumor	< .001	0.71
	Oligodendroglial tumor	.27	0.29
	Oligoastrocytic tumor	.78	−0.07
	All tumor	< .001	0.42
CHO	Astrocytic tumor	< .001	0.64
	Oligodendroglial tumor	.67	0.11
	Oligoastrocytic tumor	.44	0.19
	All tumor	< .001	0.42

Note:—Proliferation index was measured by Mib-1 labeling index. MET indicates ^{11}C-methionine; FDG, [^{18}F] fluorodeoxyglucose; CHO, ^{11}C-choline; LI, labeling index. *P* and *r* values were calculated by using Spearman correlation coefficients.

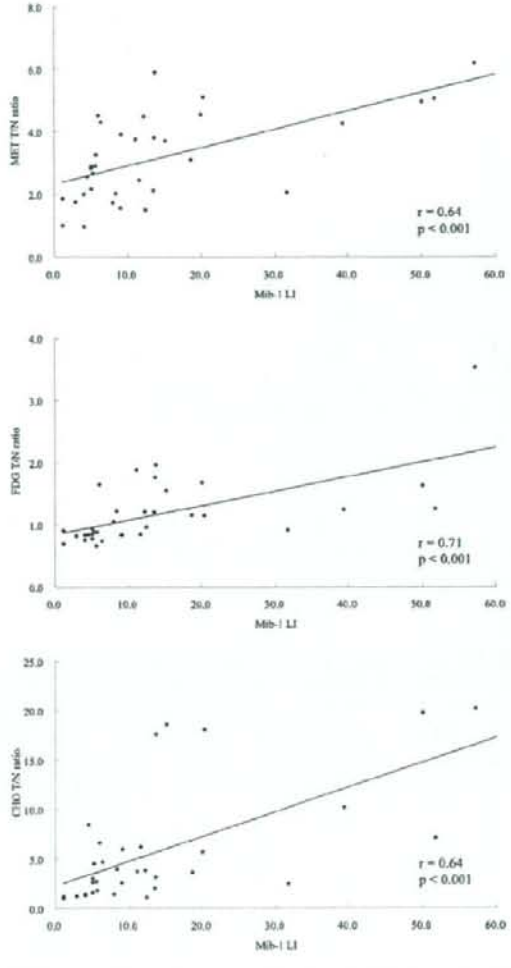

Fig 4. Graph showing the correlation between Mib-1 LI and MET T/N ratio ($r = 0.64$; $P < .001$), FDG T/N ratio ($r = 0.71$; $P < .001$), and CHO T/N ratio ($r = 0.64$; $P < .001$) in ATs.

Correlation between Tracer Accumulation and Proliferation Activity

We evaluated the proliferation activity measured by Mib-1 LI from 70 gliomas. The relationship between tracer uptake and proliferation activity is shown in Table 5. The mean Mib-1 LIs of 13 DAs, 14 AAs, 7 GBMs, 8 ODs, 9 AODs, 14 OAs, and 5 AOAs were 4.6% ± 2.1%, 14.8% ± 9.9%, 31.6% ± 20.2%, 5.5% ± 4.5%, 17.5% ± 16.6%, 7.9% ± 5.7%, and 16.1% ± 11.1%, respectively. In ATs, there were significant correlations between the T/N ratios of each tracer and the Mib-1 LI ($P <$ .001 for each; Fig 4). However, for OTs and OATs, a significant correlation was not shown in all of the tracers.

Discussion

To our knowledge, this is the first clinical study to evaluate the grade, type, and proliferation index of a series of gliomas while simultaneously assessing tumor presence by using 3 PET tracers. Previously, Kim et al[6] reported that significant differences

in glioma grades could be shown on MET PET, not on FDG PET, and that Mib-1 LI was significantly correlated with only MET uptake. Other reports have shown significant correlation between glioma grade and FDG uptake.[1,4,7,8] In our series, in the case of ATs, all of the tracers demonstrated significant positive correlations between their uptake on PET imaging and tumor grade. In addition, all 3 of the tracers demonstrated significantly positive correlations between their uptake and biologic proliferation activity as determined by Mib-1 LI. However, in neither OTs nor OATs did the uptake on PET imaging show any significant relation to grade and proliferation activity, excluding the correlation between CHO uptake and tumor grade in OTs. The T/N ratios of MET, FDG, and CHO were significantly correlated to each other in all of the gliomas except for MET and CHO in OATs. On MET PET, there was a significant difference between ATs and OTs, both in grade II and III tumors. Additionally, by ANCOVA, MET influenced both grade and type. These results show that MET has the potential to evaluate tumor grade and type and, for ATs, biologic proliferation activity.

MET and CHO are tracers that are relatively easy to use for evaluating the presence or absence of tumor on PET images compared with FDG.[22] A T/N ratio more than 2.0 means that the tumor SUV is clearly higher than that of the normal frontal cortex; therefore, the tumor is more easily visualized when the T/N ratio increases beyond 2.0. The T/N ratio of FDG was more than 2.0 in 13.7% of all gliomas. Conversely, the percentages of MET and CHO T/N ratios greater than 2.0 were 87.4% and 71.6%, respectively, in all of the gliomas, and the percentage of MET hot lesions was significantly higher than that of CHO hot lesions. These results demonstrate the significant difficulty in evaluating tumor presence on FDG PET compared with MET and CHO PET. The mean SUVs of MET and CHO in the normal frontal cortex were 1.25 ± 0.39 and 0.29 ± 0.07, respectively, in this study. Thus, the accumulation of CHO in normal brain was much lower than that of MET. However, CHO demonstrates extremely high uptake in choroid plexus, venous sinuses, and the pituitary gland, and it is difficult to recognize the existence and/or the border of brain tumor around these structures. Conversely, except for the pituitary gland, MET demonstrates slight uptake in normal brain tissue. Given these results, MET appears to be superior to CHO for evaluating tumor presence on PET.

Utriainen et al[16] investigated the association between choline accumulation and content by using 2 modalities. The association between CHO uptake measured with PET, and concentration of choline containing component measured with ^{1}H-MR spectroscopy was not statistically significant. They described that it is uncertain whether the association should be expected, because the choline-containing component measured with ^{1}H-MR spectroscopy represents intracellular metabolite pools of phosphocholine and glycerophosphocholine, whereas the rate of CHO uptake is thought to be controlled by amino acid transporter expression and attenuation in tumor endothelial cells. It is possible that there was a lack of significance in this study due to small sample size; thus, large studies using ^{1}H-MR spectroscopy and CHO PET will be necessary in the future.

Generally, OTs are reported to show significantly higher uptake of MET on PET compared with ATs. This study demonstrated results similar to previous reports.[4,23] It should be noted that the OT component can increase MET uptake of gliomas at the time of PET examination. The mean Mib-1 LI of OTs and OATs showed a general trend toward a higher proliferation index than that of ATs, even for tumors of the same grade. This finding, however, is not necessarily the only reason why the OT component leads to increased MET uptake on PET. There was no significant difference between the mean T/N ratios of tumors on MET PET between grade II and III OTs and OATs, unlike ATs, yet there was a significant difference of the mean Mib-1 LI between grades II and III OTs and OATs, similar to results seen in ATs.

Regarding the difference of MET uptake between ATs and OTs/OATs, vascular proliferation and angiogenesis of the tumor should be taken into consideration. The main mechanism of MET uptake is due to an increase of MET transport into the tumor. In gliomas, MET uptake may be attributed to the activation of the carrier-mediated transport system at the normal blood-brain barrier. This uptake does not directly reflect protein synthesis, but it represents cell avidity for amino acids.[2,24] This system may correlate with tissue proliferation, which also includes tumor angiogenesis. Plate et al[25] reported that tumors can influence the growth of their vasculature and, therefore, can regulate their increased nutrient supply, including amino acids. It has been demonstrated that expression of angiogenesis signals is an early event in glioma progression, as demonstrated by the expression of vascular endothelial growth factor (VEGF) and VEGF type 1 receptors in low-grade gliomas.[25-27] The angiogenic process initiated by the VEGF system induces an increase in carrier-mediated large amino acid transport, and the VEGF system represents the link between increased MET uptake and low-grade tumor progression.[5] In this study, the MET uptake ratio of OTs was significantly higher than the ratio of ATs of the same grade. This finding may be correlated with the microvessel attenuation of the tumor. As measured by immunostaining with factor VIII, OTs demonstrate high microvessel counts and high MET uptake comparable with malignant astrocytomas.[28] This may be one of the reasons why MET uptake of OTs is higher than that of ATs, regardless of grade.

Other authors have reported MET T/N ratio of GBMs as ranging from 2.2 to 2.5, whereas a mean SUV of normal cortex was 1.05 ± 0.46.[4,6,29,30] Hara et al[31] reported that the CHO T/N ratio of 7 cases of GBM was 11.2 ± 2.28, and mean SUV of normal posterior temporal cortex was 0.10 ± 0.02. In this article, both T/N ratios of the tumors and mean SUVs of normal cortex were higher than those of previous reports, most probably due to protocol differences.

Currently, PET-guided stereotactic brain biopsy may allow analysis of a potential correlation of metabolism with histology and confirmation of the correlation between PET tracer uptake and tumor grade. In addition, MET PET provides useful information to assess tumor spread and to plan for surgical resection and radiosurgery.[30,32-34] The limitation of this study was a lack of long-term follow-up to calculate survival rate, particularly for the cases of grade II gliomas. In addition, due to the short half-life of ^{11}C-labeled tracers, such a study necessitates the availability of an on-site cyclotron and radiopharmacy. We consider that these PET studies contribute to presurgical planning and aid in evaluating the need for post-

surgical adjuvant chemoradiotherapy in therapeutic strategies for glioma.

Conclusions

MET PET appears to be useful in evaluating grade, type, and proliferative activity of ATs. CHO PET may be useful in evaluating the potential malignancy of OTs. In terms of visual evaluation of tumor localization, MET PET is superior to FDG and CHO PET in all of the gliomas due to its straightforward detection of hot lesions. These PET studies can potentially estimate tumor viability and may be able to predict tumors with the potential for malignancy. Future studies ought to investigate the metabolic change in long-term follow-up.

Acknowledgments

We thank Prof T. Hori and Prof O. Kubo (Department of Neurosurgery, Neurologic Institute, Tokyo Women's Medical University, Tokyo, Japan) for academic support. We thank S. Fukuyama, Y Kasuya, R. Okumura, and Y. Tanaka (Kizawa Memorial Hospital, Minokamo City, Gifu, Japan) for technical support. We thank A. Mori for PET tracer production (methyl iodide synthesis and methionine module, Sumitomo Heavy Industries, Ltd, Tokyo, Japan).

References

1. Delbeke D, Meyerowitz C, Lapidus RL, et al. **Optimal cutoff levels of F-18 fluorodeoxyglucose uptake in the differentiation of low-grade from high-grade brain tumors with PET.** *Radiology* 1995;195:47–52
2. Derlon JM, Bourdet C, Bustany P, et al. **[11c]l-Methionine uptake in gliomas.** *Neurosurgery* 1989;25:720–28
3. Herholz K, Holzer T, Bauer B, et al. **11c-Methionine pet for differential diagnosis of low-grade gliomas.** *Neurology* 1998;50:1316–22
4. Kaschten B, Stevenaert A, Sadzot B, et al. **Preoperative evaluation of 54 gliomas by PET with fluorine-18-fluorodeoxyglucose and/or carbon-11-methionine.** *J Nucl Med* 1998;39:778–85
5. De Witte O, Goldberg I, Wikler D, et al. **Positron emission tomography with injection of methionine as a prognostic factor in glioma.** *J Neurosurg* 2001;95:746–50
6. Kim S, Chung JK, Im SH, et al. **11c-Methionine pet as a prognostic marker in patients with glioma: Comparison with 18f-FDG PET.** *Eur J Nucl Med Mol Imaging* 2005;32:52–59
7. Di Chiro G, DeLaPaz RL, Brooks RA, et al. **Glucose utilization of cerebral gliomas measured by [18f] fluorodeoxyglucose and positron emission tomography.** *Neurology* 1982;32:1323–29
8. Ogawa T, Inugami A, Hatazawa J, et al. **Clinical positron emission tomography for brain tumors: comparison of fludeoxyglucose f 18 and l-methyl-11c-methionine.** *AJNR Am J Neuroradiol* 1996;17:345–53
9. Tateishi U, Yamaguchi U, Seki K, et al. **Glut-1 expression and enhanced glucose metabolism are associated with tumour grade in bone and soft tissue sarcomas: a prospective evaluation by [(18)f]fluorodeoxyglucose positron emission tomography.** *Eur J Nucl Med Mol Imaging* 2006;33:683–91
10. Buck A, Schirrmeister H, Kuhn T, et al. **FDG uptake in breast cancer: Correlation with biological and clinical prognostic parameters.** *Eur J Nucl Med Mol Imaging* 2002;29:1317–23
11. Avril N, Menzel M, Dose J, et al. **Glucose metabolism of breast cancer assessed by 18f-FDG PET: histologic and immunohistochemical tissue analysis.** *J Nucl Med* 2001;42:9–16
12. Vesselle H, Schmidt RA, Pugsley JM, et al. **Lung cancer proliferation correlates with [f-18]fluorodeoxyglucose uptake by positron emission tomography.** *Clin Cancer Res* 2000;6:3837–44
13. Tian M, Zhang H, Oriuchi N, et al. **Comparison of 11c-choline PET and FDG PET for the differential diagnosis of malignant tumors.** *Eur J Nucl Med Mol Imaging* 2004;31:1064–72
14. Ohtani T, Kurihara H, Ishiuchi S, et al. **Brain tumour imaging with carbon-11 choline: comparison with FDG PET and gadolinium-enhanced MR imaging.** *Eur J Nucl Med* 2001;28:1664–70
15. Hara T, Kosaka N, Shinoura N, et al. **PET imaging of brain tumor with [methyl-11c]choline.** *J Nucl Med* 1997;38:842–47
16. Utriainen M, Komu M, Vuorinen V, et al. **Evaluation of brain tumor metabolism with [11c]choline PET and 1H-MRS.** *J Neurooncol* 2003;62:329–38
17. Schiffer D, Boasso I, Dutto A, et al. **The prognostic role of vessel productive changes and vessel density in oligodendroglioma.** *J Neurooncol* 1999;44:99–107
18. Schiffer D, Dutto A, Cavalla P, et al. **Prognostic factors in oligodendroglioma.** *Can J Neurol Sci* 1997;24:313–19
19. Cairncross JG, Ueki K, Zlatescu MC, et al. **Specific genetic predictors of chemotherapeutic response and survival in patients with anaplastic oligodendrogliomas.** *J Natl Cancer Inst* 1998;90:1473–79
20. Cairncross JG, Macdonald DR, Ramsay DA. **Aggressive oligodendroglioma: a chemosensitive tumor.** *Neurosurgery* 1992;31:78–82
21. Kapouleas I, Alavi A, Alves WM, et al. **Registration of three-dimensional MR and PET images of the human brain without markers.** *Radiology* 1991;181:731–39
22. Narayanan TK, Said S, Mukherjee J, et al. **A comparative study on the uptake and incorporation of radiolabeled methionine, choline and fluorodeoxyglucose in human astrocytoma.** *Mol Imaging Biol* 2002;4:147–56
23. Derlon JM, Petit-Taboue MC, Chapon F, et al. **The in vivo metabolic pattern of low-grade brain gliomas: a positron emission tomographic study using 18f-fluorodeoxyglucose and 11c-l-methylmethionine.** *Neurosurgery* 1997;40:276–87; discussion 287–78
24. Bustany P, Chatel M, Derlon JM, et al. **Brain tumor protein synthesis and histological grades: a study by positron emission tomography (PET) with c11-l-methionine.** *J Neurooncol* 1986;3:397–404
25. Plate KH, Breier G, Risau W. **Molecular mechanisms of developmental and tumor angiogenesis.** *Brain Pathol* 1994;4:207–18
26. Plate KH, Risau W. **Angiogenesis in malignant gliomas.** *Glia* 1995;15:339–47
27. Theurillat JP, Hainfellner J, Maddalena A, et al. **Early induction of angiogenetic signals in gliomas of gfap-v-src transgenic mice.** *Am J Pathol* 1999;154:581–90
28. Kracht LW, Friese M, Herholz K, et al. **Methyl-[11c]- l-methionine uptake as measured by positron emission tomography correlates to microvessel density in patients with glioma.** *Eur J Nucl Med Mol Imaging* 2003;30:868–73
29. Giammarile F, Cimotti LE, Jouvet A, et al. **High and low grade oligodendrogliomas (ODG): correlation of amino-acid and glucose uptakes using PET and histological classifications.** *J Neurooncol* 2004;68:263–74
30. Nariai T, Tanaka Y, Wakimoto H, et al. **Usefulness of l-[methyl-11c] methionine-positron emission tomography as a biological monitoring tool in the treatment of glioma.** *J Neurosurg* 2005;103:498–507
31. Hara T, Kondo T, Hara T, et al. **Use of 18f-choline and 11c-choline as contrast agents in positron emission tomography imaging-guided stereotactic biopsy sampling of gliomas.** *J Neurosurg* 2003;99:474–79
32. Miwa K, Shinoda J, Yano H, et al. **Discrepancy between lesion distributions on methionine PET and MR images in patients with glioblastoma multiforme: Insight from a PET and MR fusion image study.** *J Neurol Neurosurg Psychiatry* 2004;75:1457–62
33. Levivier M, Massager N, Wikler D, et al. **Use of stereotactic PET images in dosimetry planning of radiosurgery for brain tumors: clinical experience and proposed classification.** *J Nucl Med* 2004;45:1146–54
34. Pirotte B, Goldman S, Dewitte O, et al. **Integrated positron emission tomography and magnetic resonance imaging-guided resection of brain tumors: a report of 103 consecutive procedures.** *J Neurosurg* 2006;104:238–53

Acta Neurochir (2006) [Suppl] 98: 67–75

Printed in Austria

Usefulness of intraoperative magnetic resonance imaging for glioma surgery

Y. Muragaki[1], H. Iseki[1,2], T. Maruyama[2], T. Kawamata[2], F. Yamane[2], R. Nakamura[1], O. Kubo[2], K. Takakura[1], and T. Hori[2]

[1] Faculty of Advanced Techno-Surgery, Institute of Advanced Biomedical Engineering and Science, Graduate School of Medicine, Tokyo Women's Medical University, Tokyo, Japan
[2] Department of Neurosurgery, Neurological Institute, Tokyo Women's Medical University, Tokyo, Japan

Summary

Background. Radical resection of gliomas can increase patient's survival. There is known concern, however, that aggressive tumour removal can result in neurological morbidity. The objective of the present study was to evaluate the usefulness of low magnetic field strength (0.3 Tesla) open intraoperative magnetic resonance imaging (iMRI) for complete resection of glioma with emphasis on functional outcome.

Methods. From 2000 to 2004, 96 patients with intracranial gliomas underwent tumour resection with the use of iMRI in Tokyo Women's Medical University. There were 50 men and 46 women; mean age was 39 years. Tumour volume varied from 1.2 ml to 198 ml (median: 36.5 mL). Resection rate and postoperative neurological status were compared between control group (46 cases, operated on during the initial period after installation of iMRI), and study group (50 most recent cases, in whom surgery was done using established treatment algorithm and improved image quality).

Findings. Overall, mean resection rate was 93%, and medial residual tumour volume was 0.17 ml. Total tumour removal was achieved in 44 cases (46%). Compared to control group, resection rate in the study group was significantly higher (91% vs. 95%; $P < 0.05$), whereas residual tumour volume was significantly smaller (1.7 mL vs. 0.025 mL; $P < 0.001$). Nine patients in the control group (20%) and 24 in the study group (48%) experienced temporary postoperative neurological deterioration ($P < 0.01$), however, the rate of permanent morbidity evaluated 3 months after surgery did not differ significantly between the groups investigated (13% vs. 14%).

Conclusions. Use of iMRI during surgery for intracranial gliomas permits to attain aggressive tumour resection with good functional outcome. Nevertheless, surgical experience with the iMRI system, establishment of treatment algorithm, and improvement of image quality are of paramount importance for optimal results.

Keywords: Glioma; surgery; outcome; intraoperative MRI; intraoperative neuronavigation; intraoperative brain mapping.

Introduction

Gliomas are the most frequent primary brain tumours, management of which is extremely challenging. Despite advances in modern treatment modalities, including resective surgery, radiotherapy, chemotherapy, and immunotherapy, outcomes of patients with malignant gliomas remain poor. Furthermore, there is still significant controversy with regard to the goals of surgical resection [12, 25]. Some believe that since the relationship between resection rate and patient prognosis has not yet been established [7, 23], the possible benefit of radical removal of tumour is overshadowed by the relatively high risk of postoperative neurological morbidity. At the same time others argue that correlation between resection rate and prognosis has sufficiently been defined [1, 8, 14, 15] and that total tumour removal is the most effective treatment for malignant glioma.

Regardless of this controversy, most investigators agree that better demarcation of the tumour border in the eloquent areas of the brain would result in an increased resection rate with reduced risk of postoperative neurological deterioration. The objective of the present study was to evaluate the usefulness of low magnetic field strength (0.3 Tesla) open intraoperative magnetic resonance imaging (iMRI) for complete resection of glioma with emphasis on functional outcome.

Methods and materials

From 2000 to 2004, 244 neurosurgical procedures with the use of iMRI were performed in Tokyo Women's Medical University. Ninety-six patients had resection of intracranial glioma and these cases were selected for the present retrospective analysis. The vast majority of procedures were performed by the same neurosurgeon with subspecialization in surgical neuro-oncology (Y.M.). Informed consent was obtained before surgery from each patient and his/her nearest family member. Resection rate and postoperative neuro-

Table 1. *General clinical characteristics of 96 patients with intracranial gliomas operated on with the adjunct of the iMRI system*

Case characteristics	Total cohort (N = 96)	Comparative subgroups		P-value
		Control group (N = 46)	Study group (N = 50)	
Mean age ± SD (years)	39 ± 16	39 ± 18	40 ± 15	P = 0.78*
Gender (men/women)	50/46	22/24	28/22	P = 0.43**
Tumour (initially diagnosed/recurrent)	66/30	26/20	40/10	**P = 0.04****
Tumour WHO histological grade				P = 0.25**
– I	3 (3%)	2 (4%)	1 (5%)	
– II	27 (28%)	10 (22%)	17 (34%)	
– III	33 (34%)	15 (33%)	18 (36%)	
– IV	30 (31%)	16 (35%)	14 (28%)	
Tumour functional grade§				P = 0.39**
– I	16 (17%)	7 (15%)	9 (18%)	
– II	29 (30%)	17 (37%)	12 (24%)	
– III	51 (53%)	22 (48%)	29 (58%)	
Median tumour volume in mL (95% CI)	36.5 (28.7–43.9)	35.5 (19.8–46.1)	41.3 (26.7–52.4)	P = 0.52*

* According to Student's t test; ** according to chi-square test; bold: statistically significant difference ($P < 0.05$), § Sawaya functional grade: grade I (non eloquent), grade II (near eloquent), grade III (eloquent) [26].

logical status were compared between control group (46 cases, operated on during initial period after installation of iMRI), and study group (50 most recent cases, in which surgery was done using established treatment algorithm and improved image quality).

General clinical characteristics

General clinical characteristics of patients are presented in Table 1. There were 50 men and 46 women; mean age was 39.0 years (range: from 6 to 78 years). Initially-diagnosed neoplasms were found in 66 cases, whereas recurrent neoplasms were seen in 30. Sixteen tumours (17%) were located in the non-eloquent areas of the brain (Sawaya functional grade I) [26], 29 (30%) in near eloquent areas of the brain (Sawaya functional grade II), and 51 (53%) in eloquent areas of the brain (Sawaya functional grade III) [26]. The tumour volume varied from 1.2 ml to 198 ml (median: 36.5 ml).

Typing and grading of gliomas were done according to criteria of the World Health Organization (WHO) classification. There were 29 glioblastomas multiforme, 19 anaplastic astrocytomas, 15 diffuse astrocytomas, 7 anaplastic oligoastrocytomas, 6 oligodendrogliomas, 5 oligoastrocytomas, 4 pilocytic astrocytomas, 3 pleomorphic xanthoastrocytomas, 2 anaplastic ependymomas, 2 ependymomas, and one subependymoma. Three tumours (3%) corresponded to WHO grade I, 27 (28%) to grade II, 33 (34%) to grade III, and 30 (31%) to grade IV. In 3 recurrent cases histological typing and grading of tumour were not possible due to presence of extensive radiation necrosis.

Intraoperative MRI and MR compatible operating devices

The internal organization of our "intelligent operating theatre" is presented on Fig. 1A. MRI was selected as an intraoperative imaging method, because it provides excellent spatial resolution without radiation exposure [13]. Intraoperative MRI scanner (AIRIS II, Hitachi Medical, Tokyo, Japan, Fig. 1B), as available at Tokyo Women's Medical University, has a disc-shaped permanent magnet with a magnetic field strength of 0.3 Tesla and a gantry gap of 43 cm in width. Low magnetic field strength creates narrow 5-gauss line, and the patient can easily be moved outside of the field but still remaining in the operative theatre, which permits to use some conventional surgical devices (for example, high-speed drill). Nevertheless, all surgical devices and instruments that are used within the 5-gauss line, such as operating table (MOT2000-MRI, Mizuho Ikakohgyo, Tokyo, Japan, Fig. 1C) and operating microscope (MRI-30, Mitaka Kohki, Tokyo, Japan, Fig. 1D), are constructed from non-ferromagnetic material to prevent accidents and avoid image artifacts.

Body coils for the scanning of the abdominal region were used as receiver coil in the control group, while original coils for the scanning of open brain surgery with higher signal-to-noise ratio were developed later on (Head Holder Coil, Hitachi Medical, Tokyo, Japan, Fig. 1E) and used in the study group. Although the field strength of this scanner is low, it can provide images of sufficient quality for identification of residual tumours, and allows generation of 3-D reconstruction images, magnetic resonance angiography (MRA), and cine-MRI.

During surgery MR images were obtained at 3-mm slice thickness (1.5-mm slice intervals, 100 slices) under the following conditions: field of view (FOV), 230 × 230 mm; TR, 27 msec; TE, 10 msec (for T_1-weighted spin echo), and FOV, 230 × 230 mm; TR, 3000 msec; TE, 120 msec (for T_2-weighted turbo). An MRI contrast agent (gadolinium diethylenetriamine pentaacetic acid) was administered intravenously at 0.2 ml/kg in the control group and at 0.4 ml/kg in the study group. Scanning duration was 3 min and 36 sec for T_1-weighted images and 5 min for T_2-weighted images. All MRI data were displayed on the in-room display screen.

Intraoperative "real-time" update neuronavigation

A surgical navigation system (PRS navigator, Toshiba, Tokyo, Japan, Fig. 1F) was used in 35 recent cases to facilitate tumour removal and detection of its remnants. The navigator was based on a conventional infrared location-identification device, which shows the location of the suction tip and position of the suction tube in 3 sectional planes. Navigation DICOM format files of MR images were transferred to a computer through a local area network. Images were available for use in less than 5 minutes after MR scanning.

Surgical procedure

In 84 cases surgery was performed with patients in the supine position, whereas 12 patients were in prone position. After induction of

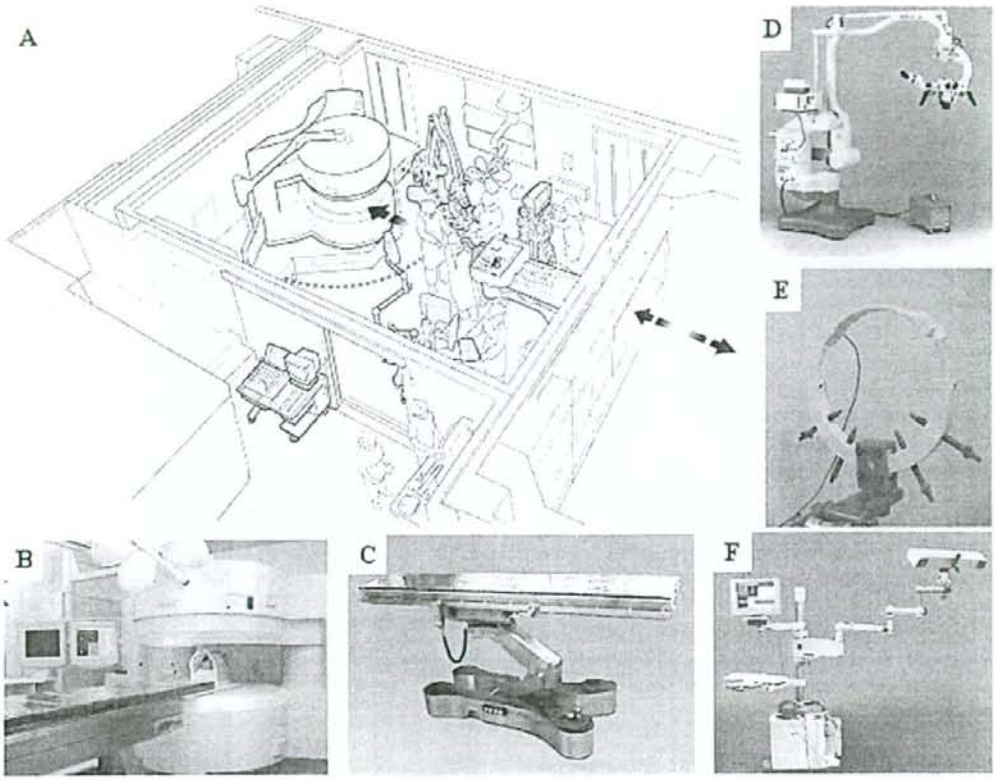

Fig. 1. The internal organization of the "intelligent operating theatre" at the Tokyo Women's Medical University: general view (A) with marked 5-gauss line (*dotted line*), 0.3 Tesla open iMRI (B), MR-compatible operating table (C), MR-compatible operating microscope (D), original receiving coil for scanning of open brain surgery (E), surgical neuronavigation system (F)

anesthesia, the patient head was fixed in a four-point head holder coil. Craniotomy was performed in a usual manner, followed by opening of the dura mater and arachnoid. Thereafter, fiducial markers were fixed to the skull, the covering coil was connected to the four-point head holder coil, and the operating table was covered with the second transparent drape. Patient's head was moved in the center of the MRI gantry by sliding the upper portion of the operating table. MR imaging was performed, and data were transferred onto a computer for further neuronavigation. The fiducial markers were registered in the computer, which permitted use of "real-time" update neuronavigation during tumour removal.

If the tumour was located near or in eloquent brain areas, cortical mapping, neurophysiological monitoring, and/or stimulation of the cranial nerves were performed – as appropriate before resection of neoplasm – for identification of the motor area, speech area, cranial nerves and its nuclei. Somatosensory evoked potentials (SEP) and motor evoked potentials (MEP) were routinely monitored during surgery.

After removal of the neoplasm, iMRI was performed again to assess the completeness of tumour resection, identification of the residual neoplasm or possible adverse effects such as haemorrhage. If residual tumour was identified and considered suitable for additional resection, the newly obtained MRI data were transferred to the navigation computer and further resection of the neoplasm was performed using this updated information. When resection of the tumour was completed, final iMRI was done to evaluate the resection rate.

Such treatment algorithm permitted us a more precise orientation in the operative field compared to conventional neuronavigation systems, which are based on MR images obtained before surgery and constitute a risk for possible mislocalization errors due to brain shift after removal of CSF and the tumour itself [18, 19].

Outcome evaluation

Comparative evaluation of neurological signs and symptoms was done before surgery, within 2 weeks after tumour resection, and 3 months thereafter.

Comparison of pre- and post-operative MRI was performed to assess resection rate and residual tumour volume. The latter was

defined as an area of increased signal intensity on contrast-enhanced T_1-weighted images [28], or, if the tumour did not show contrast enhancement, as an area of increased signal intensity on T_2-weighted images corresponding to the defined mass lesion. An area of abnormal signal intensity was computed for each slice and multiplied by the slice width (1.5 mm), and a cumulative value was obtained by adding the values for the individual slices.

Statistics

Statistical analysis was performed using Statview 5.0 (SAS Institute, Cary, NC). The level of significance was determined at $P < 0.05$.

Results

In all cases second iMRI permitted to identify the residual tumour, and additional resection was performed whenever possible (Figs. 2 and 3). If according to intraoperative brain mapping or neurophysiological monitoring the residual tumor infiltrated eloquent brain structures, it was left *in situ*. Overall, total tumour removal was achieved in 44 cases (46%), mean resection rate was 93 ± 10%, and median residual tumour volume was 0.17 ml (95% CI: 0–0.93 mL) (Table 2). Residual tumour volume was greater in neoplasms of higher histological and functional grade, but such trends did not reach statistical significance (Wilcoxon signed-ranks test or ANOVA).

Early surgical complications included 2 cases of wound infection (2%) (Table 3). No case of postoperative haemorrhage occurred. Immediately after surgery 16 patients (17%) showed improvement in pre-existing signs and symptoms, 63 (66%) remained unchanged, whereas 33 (34%) exhibited more or less prominent neurological deterioration. Therefore, total short-term morbidity was 36%.

At 3 months the neurological status of 13 patients (14%) still remained worse than before surgery. In long-term follow-up one patient died due to infection, while another one exhibited deep pulmonary embolism. Therefore, total long-term morbidity was 14% and mortality 2%.

A comparison of the two groups of patients revealed their compatibility in clinical characteristics. At the same time, resection rate in the study group compared to control group was significantly higher (91% vs. 95%; $P < 0.05$), whereas residual tumour volume was significantly smaller (1.7 mL vs. 0.025 mL; $P < 0.01$) (Table 2). The number of cases with total removal was also higher in the study group as compared to the control group (52% vs. 39%), but this difference did not reach statistical significance. Further subgroup analysis showed that residual volume of WHO grade IV tumours (4.6 ml vs. 0.05 ml; $P < 0.05$) and neoplasms of Sawaya functional grade III, located in

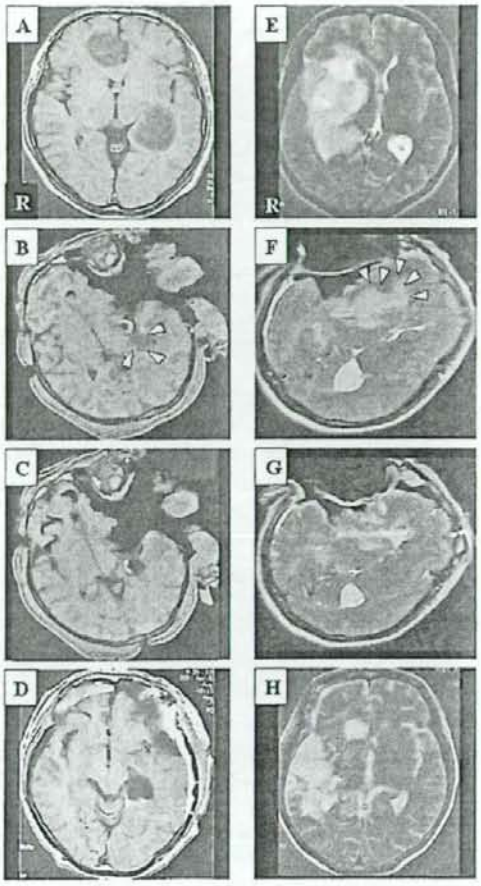

Fig. 2. Identification of residual tumor by iMRI and its further aggressive resection. In Case 1 (*left column*) primary multiple cerebral astrocytomas in the right frontal lobe and left (dominant) hippocampus (A) were removed during surgery, but residual tumour in the left hippocampal tail (*arrowhead*) was disclosed by control iMRI (B), and was removed thereafter (C) with total removal confirmated on postoperative MRI (D); the patient had transient aphasia but no permanent neurological deficit. In Case 2 (*right column*) a giant glioblastoma in the right fronto-temporal lobe, insular cortex and basal ganglia (E) was removed during surgery, but residual tumour (*arrowhead*) in the insular cortex and deep frontal lobe was identified (F) and subtotally (97%) removed (G), which was confirmed by postoperative MRI (H); the patient did not have motor deficit after surgery

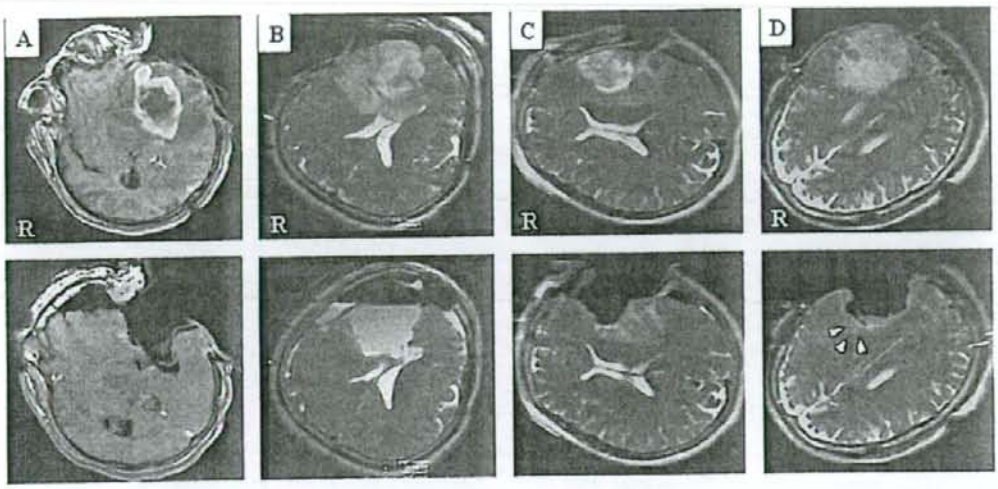

Fig. 3. iMRI before (*upper row*) and after (*lower row*) aggressive resection of gliomas located in or near eloquent brain areas: 99% removal of malignant (WHO grade IV) tumour from the left temporal lobe and insular cortex (A); 100% removal of the tumour (WHO grade II) with contralateral extension through the corpus callosum (B); 97% removal of the tumour (WHO grade III) located in the Broadmann area 44 (classical Broca zone) (C); 98% removal of the tumour (WHO grade III) located in the right parietal lobe in the vicinity of the pyramidal tract (D) with preservation of functionally important brain tissue (*arrowhead*)

the eloquent areas of the brain (3.8 ml vs. 0.23 ml, $P < 0.05$), as well as resection rate of the latter (88% vs. 95%, $P < 0.05$) were significantly improved in the study group compared to the control group (Table 2).

Nine patients in the control group (20%) and 24 in the study group (48%) experienced temporary postoperative neurological deterioration ($P < 0.05$) (Table 3). However, the rate of permanent morbidity, which was evaluated 3 months after surgery, did not differ significantly between the groups investigated (13% vs. 14%) (Table 3).

Discussion

Using intraoperative MRI

First iMRI systems were introduced in 1997 by Black *et al.* [3] and Tronnier *et al.* [32, 36]. Since then, such devices have been used for real-time observation of surgical manipulations, for assessment of the extent of tumour resection, and evaluation of the intraoperative complications. Different modifications include a twin theatrer system developed by Tronnier and Steinmeier *et al.* [29, 32], a rotatable patient table system introduced by Rubino *et al.* [24], a ceiling-mounted movable MR gantry system presented by Sutherland *et al.* [30], and high-field (1.5-Tesla) hamburger-type MR gantry system used by Nimsky *et al.* [21]. While intraoperative observation and guidance of surgery by iMRI are theoretically presumed to produce the most favorable outcomes, the available devices usually provide relatively narrow working space and necessitate all surgical devices and instruments to be composed of non-ferromagnetic materials. By contrast, systems that employ MR imaging at some temporary break points during surgical procedure, while labor and time increase for patient transfer to the MRI venue, can provide a higher degree of freedom to the surgeon and permit to use standard (not MR-compatible) surgical instruments. It should be noted that any type of iMRI system increases the operation time, because MR imaging by itself is a time-consuming process.

Hadani *et al.* [11] previously reported experience with compact mobile 0.15 Tesla MRI. Such system has definite advantages in terms of cost-performance, but needs a special magnetic shield to prevent artifacts and limits space for surgical manipulations due to narrow MR gantry gap. On the other hand, high magnetic field strength iMRI scanners can provide higher image

Table 2. *Surgical outcome in 96 cases of intracranial gliomas operated on with the adjunct of the iMRI system*

Surgical outcome parameters	Total cohort (N = 96)	Comparative subgroups		P-value
		Control group (N = 46)	Study group (N = 50)	
Median residual tumour volume in ml (95% CI)	0.17 (0–0.96)	1.6 (0–4.2)	0.025 (0–0.67)	**P = 0.006***
Median residual tumour volume in ml in regard to WHO histological grade:				
– II	0	0	0	P = 0.10*
– III	0.91	1.6	0.88	P = 0.37*
– IV	0.13	4.6	0.05	**P = 0.02***
Median residual tumour volume in mL in regard to Sawaya functional grade:				
– I	0	0	0	P = 0.07*
– II	0	0.2	0	P = 0.32*
– III	0.93	3.8	0.23	**P = 0.02***
Mean resection rate ± SD (%%)	93 ± 10	91 ± 11	95 ± 10	**P = 0.04***
Mean resection rate (%%) in regard to WHO histological grade:				
– II	94	93	96	P = 0.41*
– III	96	94	97	P = 0.11*
– IV	90	88	92	P = 0.43*
Mean resection rate (%%) in regard to Sawaya functional grade:				
– I	97	93	100	P = 0.06*
– II	94	95	94	P = 0.84*
– III	92	88	95	**P = 0.03***
Number of cases of total removal	44 (46%)	18 (39%)	26 (52%)	P = 0.21**

* According to Student's t test; ** according to chi-square test; bold: statistically significant difference ($P < 0.05$).

Table 3. *Functional outcome after removal of intracranial gliomas with the adjunct of the iMRI system*

	Total cohort (N = 96)	Comparative subgroups		P-value
		Control group (N = 46)	Study group (N = 50)	
Neurological status				
– improved	16 (17%)	11 (24%)	5 (10%)	P = 0.68**
– unchanged	63 (66%)	26 (57%)	37 (74%)	P = 0.07**
– temporary deteriorated	33 (34%)	9 (20%)	24 (48%)	**P = 0.01****
– permanently deteriorated	13 (14%)	6 (13%)	7 (14%)	P = 0.04**
Surgical complications				
– infection	2 (2%)	2 (4%)	0 (0%)	P = 0.14**
– postoperative haemorrhage	0 (0%)	0 (0%)	0 (0%)	–
– venous embolism	1 (1%)	0 (0%)	1 (2%)	P = 0.99**
– pulmonary embolism	1 (1%)	0 (0%)	1 (2%)	P = 0.99**
Total short-term morbidity	35 (36%)	11 (24%)	24 (48%)	**P = 0.01****
Total long-term morbidity	13 (14%)	6 (13%)	7 (14%)	P = 0.89**
Total mortality	2 (2%)	1 (2%)	1 (2%)	P = 0.95**

* According to Student's t test; ** according to chi-square test; bold: statistically significant difference ($P < 0.05$).

quality, shorter scanning time, and variability of imaging options, such as diffusion tensor imaging [20], functional MRI [10], and proton MRS. Image distortion during scanning, however, can cause geometric errors, which can result in suboptimal conditions for neuronavigation during tumour removal. Risk of image distortion is 5 times greater in 1.5 Tesla MR scanner compared to 0.2 Tesla one [9]. It should be also taken into